Daily rhythms in the transcriptomes of the human parasite *Schistosoma mansoni*

Kate A. Rawlinson[1*], Adam J. Reid[1], Zhigang Lu[1], Patrick Driguez[1,2], Anna Wawer[3], Avril Coghlan[1], Geetha Sankaranarayanan[1], Sarah Kay Buddenborg[1], Carmen Diaz Soria[1], Catherine McCarthy[1], Nancy Holroyd[1], Mandy Sanders[1], Karl Hoffmann[3], David Wilcockson[3], Gabriel Rinaldi[1], Matt Berriman[1*]

[1]Wellcome Sanger Institute, Wellcome Genome Campus, Hinxton, CB10 1SA, UK.
[2] King Abdullah University of Science and Technology, Thuwal, Makkah, Saudi Arabia
[3] Institute of Biological, Environmental, and Rural Sciences, Aberystwyth University, Aberystwyth SY23 3DA, UK

* Corresponding authors: kr16@sanger.ac.uk and mb4@sanger.ac.uk

Abstract

The consequences of the earth's daily rotation have led to 24-hour biological rhythms in most organisms. Parasites have daily rhythms, which, when in synchrony with host rhythms, optimize their fitness. Using round-the-clock transcriptomics of male and female *Schistosoma mansoni* blood flukes we have discovered the first 24-hour molecular oscillations in a metazoan parasite, and gained insight into its daily rhythms. We show that expression of ~2% of its genes followed diel cycles. Rhythmic processes, in synchrony in both sexes, included a night-time stress response and a day-time metabolic 'rush hour'. These 24hr rhythms may be driven by host rhythms and/or generated by an intrinsic circadian clock. However, canonical core clock genes are lacking, suggesting an unusual oscillatory mechanism or loss of a functional clock. The daily rhythms in biology identified here, may promote within-host survival and between-host transmission, and are important for the development and delivery of therapeutics against schistosomiasis.

Key words: daily rhythms, transcriptomics, RNA-seq, adult *Schistosoma mansoni,* animal circadian clock genes

Introduction

Most organisms have biological rhythms that coordinate activities with the consequences of the earth's daily rotation (Reese *et al*., 2017). These biological rhythms are driven by daily cycles in environmental factors such as temperature, light, predation risk and resource availability, as well as an endogenous molecular circadian clock (Rund *et al*., 2016). Whereas some daily phenotypes are driven by natural environmental cycles, circadian rhythms persist in constant conditions, sustained by an endogenous oscillatory mechanism, the circadian clock. The circadian clock is a molecular network that in animals is largely conserved across diverse lineages (Hardin, 2011; Takahashi, 2017). Interconnected regulatory loops are organized around a core transcriptional-translational feedback loop consisting of the positive factors including *CLOCK*, *ARNTL* (*BMAL1/CYCLE*) and the negative regulators *TIMELESS*, *CRYPTOCHROME* and *PERIOD*, and secondary clock genes that modulate the effects of the core feedback loop; together these drive oscillations in many clock-controlled genes. Circadian and clock-controlled genes are a subset of the genes that show daily

patterns of expression (diel genes), and all together they lead to 24-hour patterns in physiology and behaviour.

Much like their free-living counterparts, parasites living within the bodies of other organisms also have biological rhythms. These rhythms maximise parasite fitness in terms of within-host survival and between-host transmission (O'Donnell *et al*., 2011). Understanding the rhythms of parasites will provide insight into how they temporally compartmentalise their internal processes and host interactions to survive the daily cycles of host immune system activity and physiology. Furthermore, understanding both parasite and host rhythms may enable development of vaccines and drugs that take advantage of rhythmic vulnerabilities in parasites or harness host rhythms to improve efficacy and reduce drug toxicity (Westwood *et al*., 2019). Recent work on blood-dwelling protozoan parasites has revealed daily rhythms in gene expression, physiology, drug sensitivity (Rijo-Ferreira *et al*., 2017) and the presence of an intrinsic clock (Rijo-Ferreira *et al*., 2020). However, similar studies on metazoan parasites are lacking. Exploring daily molecular oscillations in metazoan parasites will give us insight into how these longer-lived organisms can survive host daily cycles over a life-span of many years, and will lead to an understanding of how animal circadian clockwork has evolved in parasites.

One long-lived metazoan parasite is *Schistosoma mansoni*, a blood-dwelling flatworm (Platyhelminthes), that can live in the vascular system for over 30 years (Harris *et al*., 1984). It causes Schistosomiasis, a major neglected tropical disease, that has a profound human impact, with an estimated 140,000 cases and 11,500 deaths in 2019 (GBD 2019). Nothing is known about whether the adult worms (which give rise to the pathology-causing eggs) exhibit any daily or circadian rhythms in any aspect of their biology because they live deep inside the portal veins. Earlier in development *S. mansoni* cercariae larvae are shed from the snail host at a population-specific time of day (Mouahid *et al*., 2012), but the molecular underpinnings of this rhythm are not known. *S. mansoni* naturally infects both humans and mice in the wild (Catalano *et al*., 2018), and mice are commonly used as definitive hosts in the laboratory maintenance of its life cycle. The mouse is also the model species routinely used to study circadian rhythms in mammals (Zhang *et al*., 2014), and because of this, we know there are many daily rhythmic fluctuations in the vasculature (e.g. temperature, pressure, oxygen, glucose, red and white blood cells [Damiola *et al*., 2004, Curtis *et al*., 2007, Scheiermann *et al*., 2012, Adamovich *et al*., 2017, Llanos & de Vacarro, 1972]) that may act as zeitgebers (German for "time giver" or synchronizer) to influence the worm's biology and potentially its rhythms. Here we ask whether sexually mature male and female *S. mansoni*, collected from their natural environment (the mesenteric vasculature of mice) under

82 ‘normal’ host conditions (Light:Dark cycle) show daily rhythms in their transcriptomes. Transcripts
83 that cycle with 24 hour periodicity (diel or cycling genes), were identified using RNA-seq time
84 series from female and male worms as well as the heads of males (to enrich for the worm’s cephalic
85 ganglia or ‘brain’; the site of the master circadian clock in some animals). Protein function
86 databases and published single cell RNA-seq data (Wendt *et al*., 2020) were interrogated using our
87 diel genes to identify rhythmic biological processes. One-to-one orthologs were compared between
88 *S. mansoni* diel genes and those of other animals to investigate metazoan circadian clock
89 components. Having found that most cell types associated with the female reproductive system are
90 enriched for cycling genes, we show that egg laying *in vitro* oscillates between day and night. Our
91 discovery that genes oscillate throughout the 24-hour period has given us an understanding of the
92 fine-scale temporal partitioning of biological processes in male and female worms, and indications
93 of parasite/host interactive rhythms. As these diel genes include potential drug targets and a vaccine
94 candidate, this study will benefit the development and delivery of treatments against
95 schistosomiasis.
96

97 ## Results

98 We collected mature male and female worms at four hour intervals over a 44 hour period from mice
99 entrained in alternating 12-hour light and dark cycles (LD12:12). Although light is probably not a
100 relevant zeitgeber to schistosome adults (as penetrative light levels below 5mm in mammalian
101 bodies are minimal, Ash *et al*., 2017), light is an important cue for the mouse, and as nocturnal
102 creatures, they are active mainly during the dark phase (Jud *et al.* 2005). Zeitgeber time (ZT) 0
103 indicates the beginning of the light phase and resting phase for the mouse (which we call day-time
104 here), and ZT 12 is the beginning of dark phase and active phase for the mouse (called night-time in
105 this study). Male and female worms from each mouse were separated and pooled. Heads of male
106 worms were also isolated and these were pooled for each mouse. RNA was extracted from each
107 pool and sequenced. This gave us three time-series datasets; one for whole female worms, one for
108 whole males and one for male heads (**Figure 1A**).
109

110 ### 1. Daily rhythms in the transcriptomes of adult *Schistosoma mansoni*

111 From each dataset, we identified genes that were differentially expressed (FDR < 0.05) over a 24
112 hour period: 206 in females, 194 in males and 48 in male heads (**Supplementary Table 1-3**). We
113 then determined which differentially expressed genes were oscillating with a periodicity close to 24
114 hours using JTK_cycle (Hughes et al., 2010), and found 98 diel genes in females, 141 in males and
115 18 in male heads (**Figure 1B&C; Supplementary table 1-4**). A significant number were shared

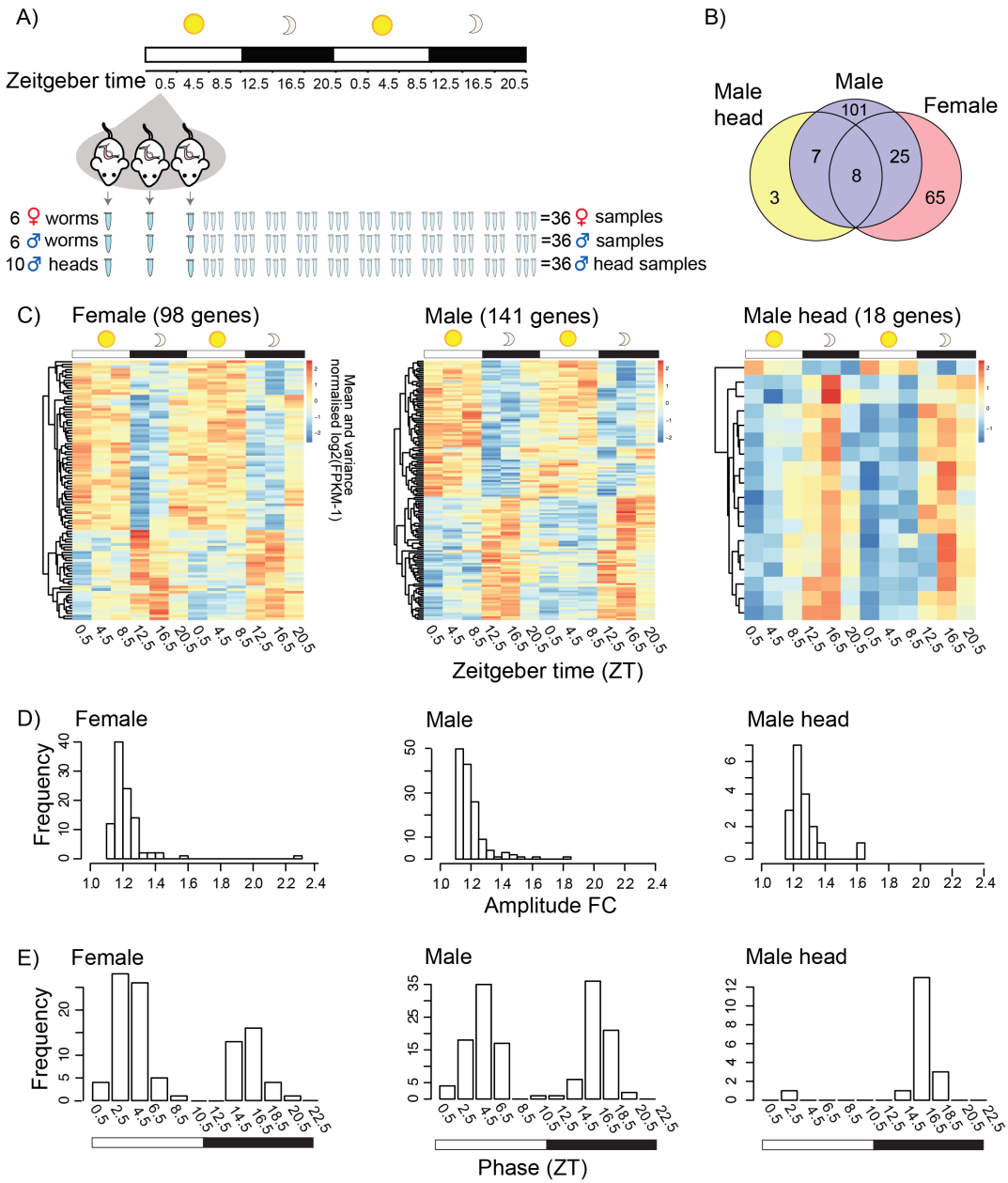

Figure 1. *Schistosoma mansoni* genes with 24-hour periodicity in their expression in adult worms. **A**) Schematic of the collection of pooled worm samples every 4 hours over 44 hours. **B**) Overlap in 209 diel genes between females, males and male heads. **C**) Expression heatmaps of diel genes. Each row represents a gene whose transcripts oscillate with ~24 hour periodicity, ordered vertically by phase. **D**) Histograms of rhythmic daily fold changes (FC) in transcript abundance. **E**) Histograms showing bimodal peaks of expression in diel genes in both sexes, but in male heads most diel genes peak at midnight.

between males and females (33; Fisher's exact test odds ratio = 47, $P < 10^{-16}$) and between males and male heads (15; Fisher's exact test odds ratio = 395, $P < 10^{-16}$; **Figure 1B, Supplementary table 4**). The combined number of diel genes from the three datasets was 209 (**Figure 1B; Supplementary table 4**), 1.9% of the *S. mansoni* (v7) gene set. The median peak-to-trough fold change (amplitude) of gene expression for diel genes was 1.19, 1.18 and 1.24 for females, males and male heads respectively. However, many genes had much higher daily fold-changes in

131 expression (**Figure 1D; Table 1**); the highest in each of the datasets were *SmKI-1* (Smp_307450,
132 fold change 1.8) in males that encodes a BPTI/Kunitz protease inhibitor domain protein, as well as
133 *hsp70* (Smp_049550, 1.6 fold) in male heads and *hsp90* (Smp_072330, 2.3 fold) in females that
134 each encode heat shock proteins (in males *Hsp90* has a 4.8 fold change but falls just outside FDR
135 <0.01 threshold [FDR = 0.0103])(**Table 1**)(see **Supplementary table 5** for orthologs in other taxa**)**.
136 While we identified rhythmic genes with peaks of expression at most times of day, there was a clear
137 bimodal pattern in both females and males (**Figure 1E**). In females, expression peaked at 2.5-4.5hr
138 (ZT) after lights on and at 14.5-16.5 hr (ZT) (2.5-4.5hr after lights off), but with 66% of the cycling
139 genes peaking during the day (the hosts resting phase), while in males the peaks occurred at 4.5 and
140 16.5 (ZT) (with a 53:47% split between light:dark phases). In the heads of males, the expression of
141 diel genes peaked at ZT 16.5, and was not bimodal, with all but one reaching peak expression
142 during the night (the hosts active phase).
143
144 **Table 1.** Diel genes with the highest expression amplitudes. Daily fold-changes in transcript
145 abundance are shown for female and male worms, plus male heads, with peak phase of expression
146 (Zeitgeber Time, ZT, grey shading= night, white = day) and significance of 24-hr rhythmicity
147 determined using JTK package. (* I-Tasser predicted structural analogue, see supplementary table
148 6).

Dataset	Gene ID	Gene description	Fold change	Phase (ZT)	JTK Benjamini-Hochberg q-value
Female	Smp_072330	Heat shock protein 90	2.30	14.5	0.00032
	Smp_326610	Trematode eggshell synthesis domain-containing protein	1.56	6.5	0.00191
	Smp_004780	FKBP-type peptidylprolyl isomerase (PPIase)	1.41	16.5	0.00019
	Smp_044850	Ribokinase	1.41	16.5	0.00770
	Smp_342000	FMRFamide-activated amiloride-sensitive sodium channel	1.38	8.5	0.00191
	Smp_069130	Heat shock protein 70 (Hsp70)-4	1.35	14.5	0.00029
	Smp_319380	n/a	1.33	2.5	0.00362
	Smp_244190	ZP domain-containing protein	1.31	14.5	0.00588
	Smp_340010	Putative eggshell protein	1.30	4.5	0.00235
	Smp_064860	Putative heat shock protein 70 (Hsp70)-interacting protein	1.30	16.5	7.92E-05
Male	Smp_307450	SmKI-1, a BPTI/Kunitz protease inhibitor domain protein	1.83	4.5	0.00311
	Smp_049550	Putative heat shock protein 70 (Hsp70)	1.62	16.5	1.21E-06
	Smp_324960	Hypothetical protein (Fatty acid synthase-like*)	1.57	18.5	0.00112
	Smp_327270	Very-long-chain 3-oxoacyl-CoA reductase	1.52	18.5	0.00763
	Smp_327260	Transmembrane protein 45B	1.49	18.5	0.00468
	Smp_013950	Solute carrier family 43 member 3	1.48	0.5	0.00112
	Smp_328570	n/a	1.48	4.5	0.00763
	Smp_327240	Hypothetical protein (GTPase activator activity*)	1.45	18.5	0.00651
	Smp_004780	FKBP-type Peptidylprolyl isomerase (PPIase)	1.36	16.5	7.31E-05
	Smp_013790	Probable ATP-dependent RNA helicase, DDX5	1.35	0.5	0.00047
Male head	Smp_049550	Putative heat shock protein 70 (Hsp70)	1.63	16.5	1.43E-05
	Smp_004780	FKBP-type peptidylprolyl isomerase (PPIase)	1.35	16.5	0.00055
	Smp_145560	Monocarboxylate transporter 9	1.33	2.5	0.00236
	Smp_124820	Putative chromosome region maintenance protein 1/exportin	1.30	18.5	0.00236
	Smp_069130	Heat shock protein 70 (Hsp70)-4	1.30	16.5	0.00236
	Smp_333170	85/88 kDa calcium-independent phospholipase A2	1.28	18.5	0.00188
	Smp_113620	Serine/arginine-rich splicing factor 2	1.27	16.5	0.00297
	Smp_049600	Putative DNAj (Hsp40) homolog, subfamily C, member 3	1.25	16.5	7.31E-05
	Smp_214080	VEZF1/Protein suppressor of hairy wing/Zld/ C2H2-type	1.25	16.5	7.49E-06
	Smp_246230	Nicotinate-nucleotide pyrophosphorylase	1.24	16.5	0.00035

149

150 **2. Putative functions of diel genes**

151 To better understand the possible function of the diel genes, we used a combination of annotation-
152 enrichment analyses based on Gene Ontology (GO), KEGG pathways, STRING molecular
153 interactions and the adult *S. mansoni* single-cell RNA-seq dataset from Wendt *et al*. (2020)
154 (**Supplementary tables 7,8,9, figure 2, supplementary figures 1 & ?**). Our analyses show that the
155 diel genes are involved in distinct rhythmic processes during the night and day time.

156

157 ***Night-time peaking genes***

158 Of the 63 genes with a night-time peak in males, 33 formed a single large network based on their
159 predicted STRING interactions (**Figure 2**). Within this network many of the molecules with the
160 largest number of interactions were putative molecular chaperones (orthologs to heat shock proteins
161 [HSPs] and their co-chaperones) involved in protein processing the ER and the stress response. In
162 females a smaller network of 13 genes was predicted, but heat shock /stress response genes were
163 still the main constituents **Supplementary figure 1**). These observations were supported by
164 enrichment of GO terms related to protein folding and chaperones: protein folding/unfolded protein
165 binding (males FDR 0.0013, females FDR 10^{-9}; **Supplementary table 7).** Diel genes involved in
166 these processes and networks all had acrophases between 14.5-18.5 ZT (i.e. mid dark
167 phase)**(Supplementary figure 2)**, and could be mapped to three KEGG pathways; 'protein
168 processing in the endoplasmic reticulum', 'PI3K-AKT signalling' and 'Estrogen
169 signalling'(**Supplementary figures 3-5**). Orthologs of six of the diel HSPs in *S. mansoni* show 24-
170 hour rhythms in other animals as well (**Supplementary tables 4, 5 and 13**).

171

172 Ten HSPs and co-chaperones cycled in both sexes, with eight oscillating in phase synchrony
173 between the sexes **(Supplementary figure 2)**. A striking example of this is seen in *hsp90*
174 (Smp_072330) and *FKBP-type peptidylprolyl isomerase (PPIase)*(Smp_004780); *hsp90* peaks at
175 the start of the dark phase, 4 hours before *PPIase* (**Figure 3 & 4).** In other animals, these proteins
176 form part of a heterocomplex that chaperones steroid hormones in cell signalling (**Supplementary**
177 **figures 5**) and they are critical for reproductive success (Cheung-Flynn et al., 2005). Although their
178 functions aren't known in *S.mansoni*, both are single cell markers for germ stem cell progeny and
179 we show, using whole mount *in situ* hybridisation (WISH), that *PPIase* is expressed in sperm
180 throughout the testes and in all oocytes in the ovary (**Figure 3C & 4C).** *PPIase* also cycles in male
181 head samples and is expressed in many cells in the head (**Figure 3C**). There were also sex
182 differences in the diel genes involved in the nightly chaperone response. For example, a *DNAj*
183 *(hsp40*), which has homologs located on the different sex chromosomes (known as

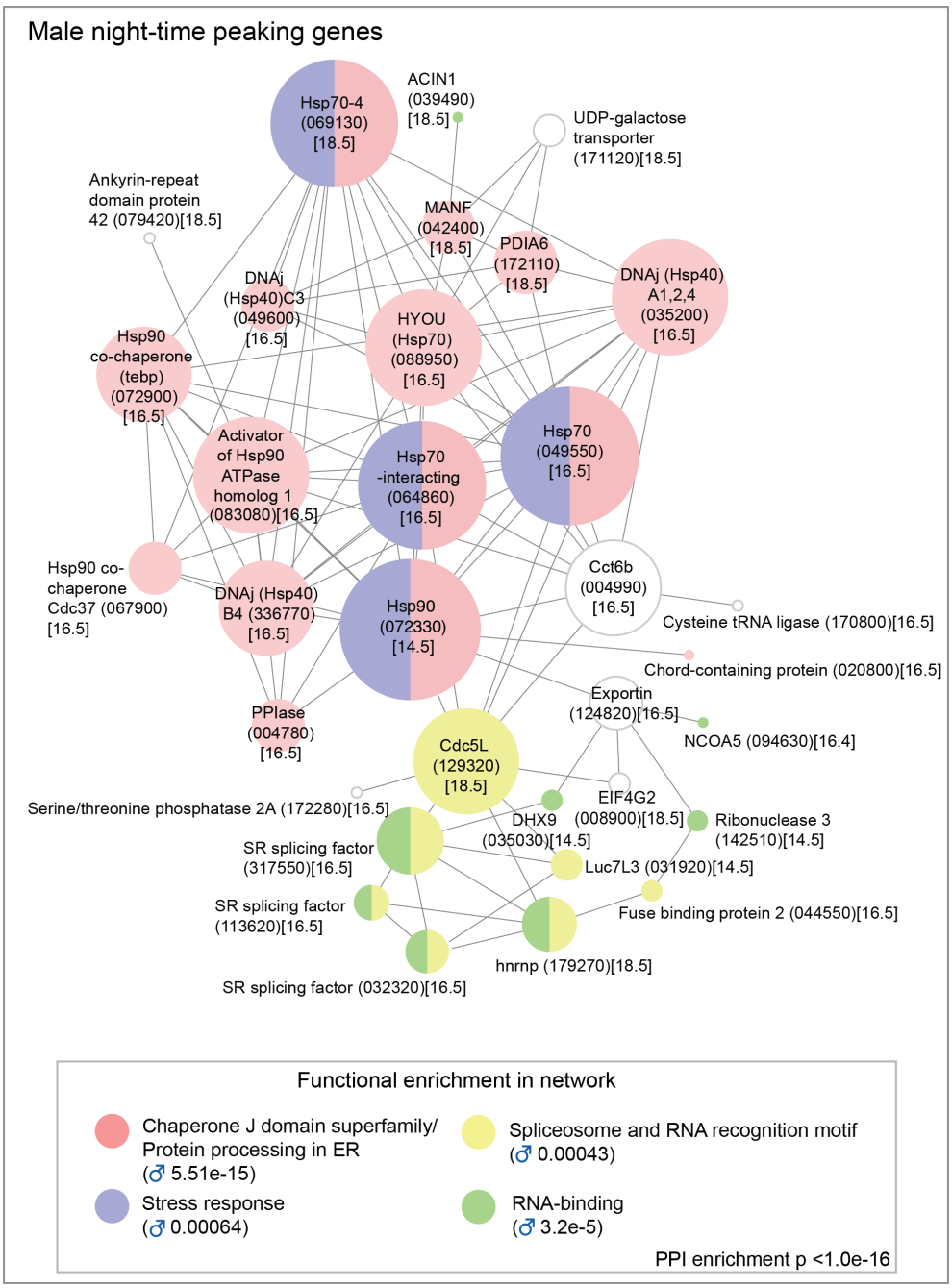

Figure 2. Predicted molecular interaction networks of night-time peaking genes in male *Schistosoma mansoni* (computed using the STRING online database). All genes peaked between 14.5-18.5 ZT (i.e. between 2.5- 6.5 hours after the start of the dark phase). Node size reflects the number of connections a molecule has within the network. Lines (edges) connecting nodes are based on evidence of the function of homologues. Functional enrichment (FDR) as provided by STRING. (PPI= predicted protein interaction; gene identifiers shown in parenthesis but with "Smp_" prefix removed for clarity; timing of acrophase (ZT) in square brackets).

gametologues)(Buddenborg *et al*., *in prep*), has diel expression in both gametologues. Schistosomes have a ZW sex chromosome system, where females are ZW and males are ZZ. The Z gametologue (Smp_336770) cycles in females, males and male heads, and the W gametologue (Smp_020920) also cycles, and is present only in females. Further sex differences included diel expression, in males only, of nine genes whose orthologs are involved in stress response and recovery

198 **(Supplementary figure 2iii)**. Four of these genes are markers for tegument-related cell types
199 **(Figures 3)** and as the male tegument forms a large surface area that is in direct contact with mouse
200 blood and endothelium, these cells are likely to be exposed to environmental heat shock triggers.

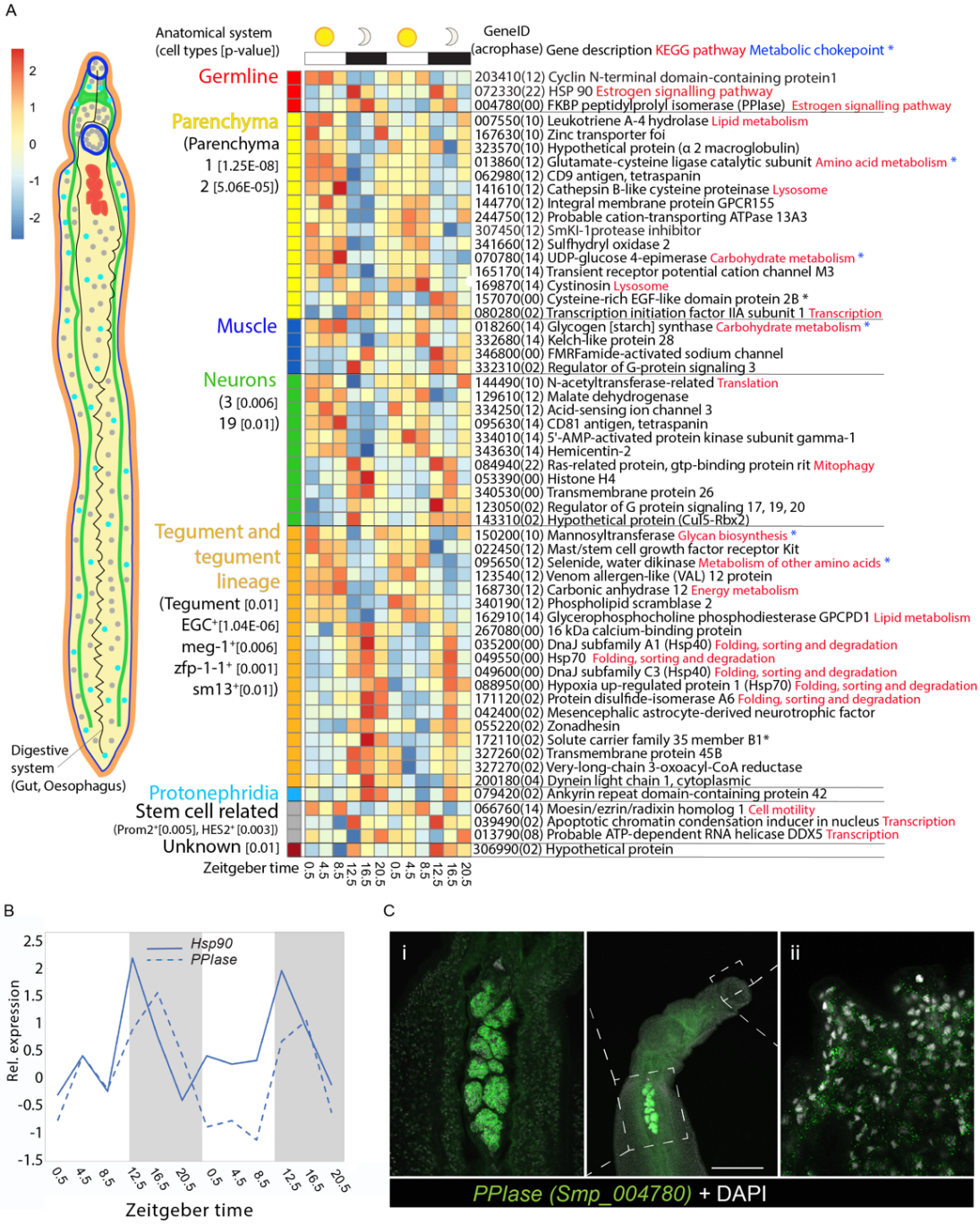

201

202 **Figure 3. A)** Heatmap of the 57 male diel genes that are single cell markers (identified in Wendt *et*
203 *al*., 2020). Each row represents a diel gene, ordered vertically by phase within anatomical systems
204 containing constituent cell types. Diel genes that are markers for multiple cell type categories are
205 placed within cell type (and their category) with greatest difference between the Seurat pct1-pct2
206 scores. "Smp_" prefixes have been removed from gene identifiers for clarity; timing of acrophase in
207 parentheses . P-value of cell types significantly enriched in diel genes given in brackets [p<0.05].
208 **B**) Temporal relative expression profiles of *Hsp90* (Smp_072330) and *FKBP-type peptidylprolyl*
209 *isomerase (PPIase)*(Smp_004780) showing peaks of expression at night. **C**) WISH expression of
210 *PPIase* showing labelled transcripts in male worm i) throughout the testes, and ii) in the head (scale
211 bar = 100μm)(100% of individuals examined, n = 10).

212 Night-time peaking genes were also associated with GO terms related to RNA binding and mRNA
213 splicing, but in males only (FDR = 0.0002 for RNA binding, FDR=0.0292 for mRNA splicing;
214 **Supplementary table 7**). Based on STRING, many of these genes form part of the night-time
215 network (**Figure 2**), including putative homologues of: *human Ser/Arg-rich splicing factors*
216 (Smp_317550, Smp_032320, Smp_113620); *heterogeneous nuclear ribonucleoprotein* (Hnrp;
217 Smp_179270): the *cell division cycle control protein Cdc5L* (Smp_129320), a spliceosome
218 component; and the splicing regulator (Li *et al*., 2013) *far upstream element-binding protein*
219 (Smp_044550). The night-time network predicts an interaction between heat shock proteins and
220 RNA-binding and mRNA splicing genes, connected via *Cdc5L* **(Figure 2)**.
221
222 Diel genes involved in regulation of GPCR functioning (*regulator of G-protein signalling 3 [RGS3]*
223 Smp_332310; and *RGS20* Smp_123050) peaked at night and are markers for muscle and nerve
224 cells respectively (**Figures 3 and 4**). *Histone 4* (Smp_053390) and *gtp-binding Ras-related protein*
225 (Smp_084940)(a member of the histone co-chaperone pathway) also peaked at night in males and
226 are markers for nerve cell types (**Figure 3)**. Neuronal activity promotes histone turnover (Maze *et*
227 *al*., 2015; Grover *et al*., 2018) and taken together these results may indicate higher sensory
228 responsiveness and activity night.
229
230 ***Day-time peaking genes***
231 Predicted interactions between the day-time peaking genes were more limited than at night; both
232 sexes had interactions of genes associated with metabolism (**Supplementary figures 6**). There were
233 32 diel genes that could be mapped to KEGG metabolic pathways; most of which are involved in
234 lipid, carbohydrate and amino acid metabolism **(Supplementary table 9)**. Of these, 28 have
235 acrophases between 0.5–6.5 ZT, suggesting a peak in metabolic activity at this time; an extended
236 metabolic 'rush hour' **(Figure 5A)**. We identified twenty-one diel genes that have previously been
237 classified as metabolic chokepoints (capable of uniquely generating specific products or utilising
238 specific substrates, International Helminths Genome Consortium, 2019) for potentially targeting
239 with new drugs, 15 of these peaked during the day (**Figure 5B**) and six at night (**Supplementary**
240 **table 4**). Several metabolic diel genes were also markers of specific cell types: those of the
241 reproductive system in female worms, and those of tegumental, parenchymal and muscle cells in
242 males (**Figures 3 & 4**).
243
244 There are four diel genes involved in the insulin signalling pathway and they all peaked between
245 2.5-6.5 ZT; *glycogen synthase* (Smp_018260) and *3-phosphoinositide-dependent protein kinase 1*
246 (Smp_094250) in males, and *hexokinase* (Smp_043030) and *protein phosphatase 1 regulatory*

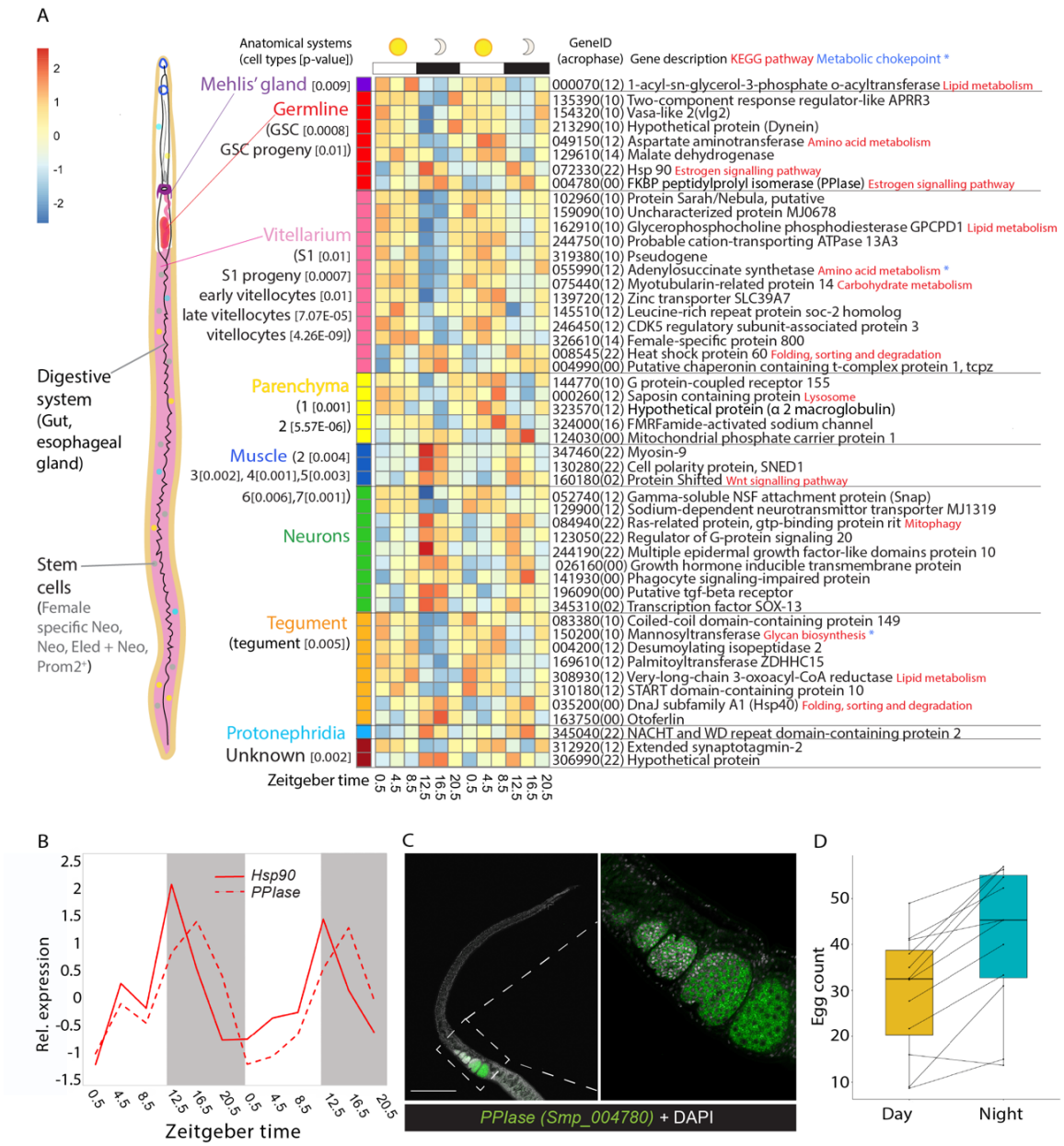

Figure 4. A) Heatmap of 48 single-cell marker genes that showed diel expression in females. Marker genes are from Wendt et al., 2020. Each row represents a diel gene, ordered vertically by phase within anatomical systems containing constituent cell types. Diel genes that are markers for multiple cell type categories are placed within cell type (and their category) with greatest difference between their Seurat pct1-pct2 scores. "Smp_" prefixes have been removed from gene identifiers for clarity; timing of acrophase in parentheses. P-value of cell types significantly enriched in diel genes given in brackets [p<0.05]. B) Temporal relative expression profiles of *Hsp90* (Smp_072330) and *FKBP-type peptidylprolyl isomerase (PPIase)*(Smp_004780) showing peaks of expression at night. C) WISH expression of *PPIase* showing labelled transcripts in female worm in all oocytes in the ovary (scale bar = 100μm)(100% of individuals examined, n = 10). D) Female (paired) worms *in vitro* lay more eggs at night (median and interquartile ranges) than during the day (n=12 female worms; median (night egg count - day egg count) = 12.0; paired Wilcoxon test: P=0.003216).

subunit 3B (Smp_167660) in females (although the latter three fell between FDR adjusted p-values of 0.01-0.05)(**Supplementary table 9, Figure 5D**).

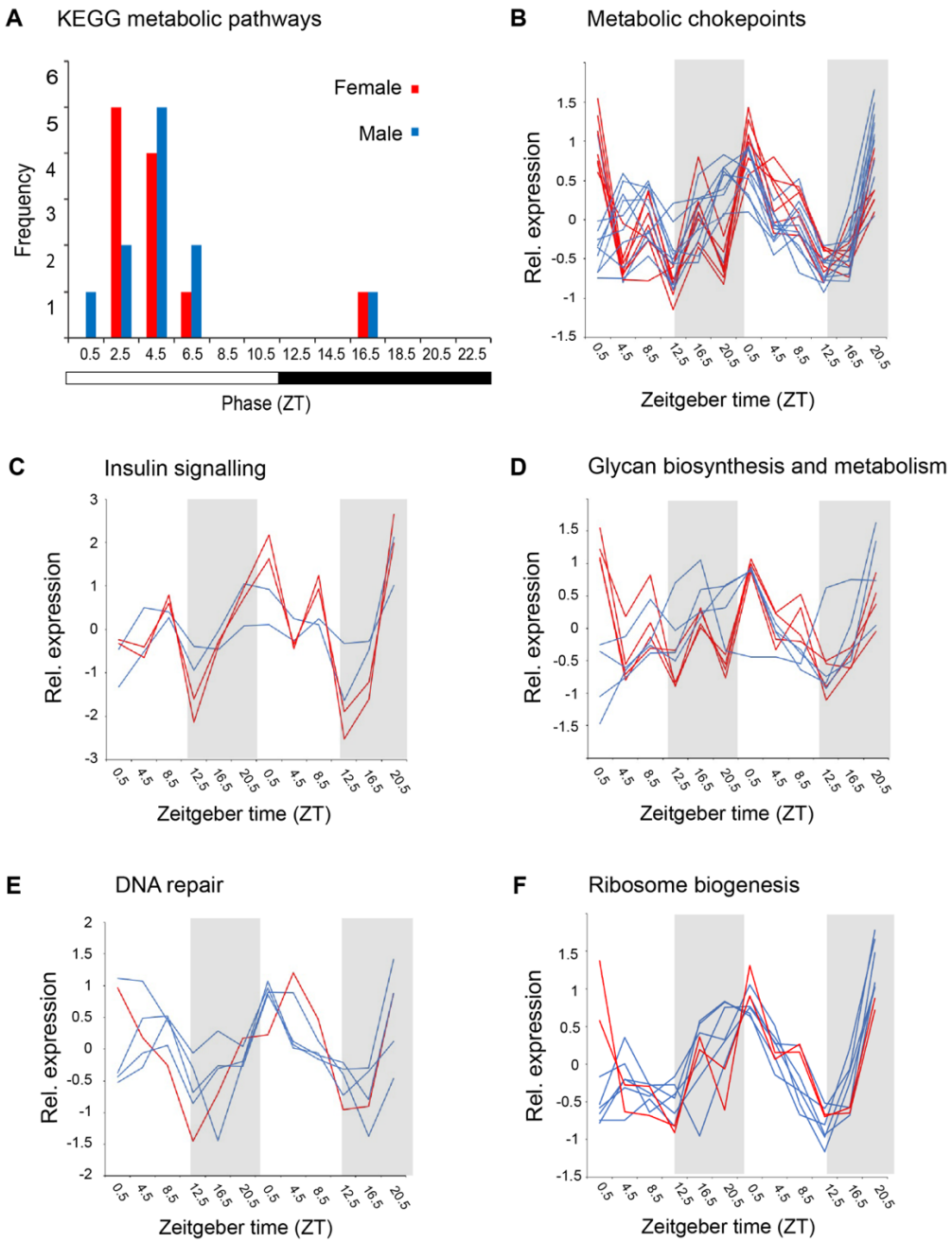

Figure 5. Light-phase peaking diel genes are involved in metabolism, DNA repair and ribosome biogenesis. **A**) Peak phase of expression of diel genes in KEGG pathways for metabolism. Temporal expression profiles of **B**) day-time peaking metabolic genes identified as chokepoints and potential drug targets, **C**) genes involved in the insulin signalling pathway **D**) genes involved in glycan biosynthesis and metabolism, **E**) DNA repair and **F**) ribosome biogenesis.

Glycans and glycoproteins that are secreted or localized to the tegument interact with the host immune and hemostatic systems (Smit *et al*., 2015). We found six diel genes involved in N-glycan and glycosaminoglycan synthesis, and glycosylation (Mickum *et al*. 2014), five of which peaked during the day (**Figure 5D, supplementary table 9**), including mannosyltransferase (Smp_150200) that is a marker for a tegumental cell type (**Figures 3 & 4; supplementary table 8**). Three others encode enzymes involved in synthesis of heparin-like glycosaminoglycans that may increase anti-coagulation activity of mammalian host blood (Mebius *et al*., 2013); putative beta-1,3-

278 glucuronyltransferase (heparin-like)(Smp_083130) and Zinc finger CCHC domain-containing
279 protein 4 (Smp_245920) peak during the day in females, whereas putative heparan sulfate n-
280 deacetylase/n-sulfotransferase (Smp_134250) cycles in males, but peaks at night **(Supplementary**
281 **table 9)**.
282
283 Also peaking during the day are other genes involved in host-parasite interactions. *SmKI-1*
284 (Smp_307450) is one of four similar genes that correspond to Smp_147730 from an earlier version
285 (v5) of the genome assembly (see additional information). The SmK1-1 protein is localised to the
286 tegument and secreted into the host where it inhibits host proteases (including neutrophil elastases)
287 involved in triggering the immune response (Morais *et al*. 2018), and interferes with host
288 coagulation pathways to delay blood clot formation (Ranashige *et al*., 2015). Smp_307450 reaches
289 its peak at midday (ZT 4.5)(**Figure 6**) a few hours before the daily increase of mouse blood
290 coagulation factors (Bertolucci *et al*., 2005) and coinciding with the day-time release of mouse
291 neutrophils into the blood from bone marrow (De Filippo & Rankin, 2018), possibly indicating that
292 its diel expression may be anticipating or responding to these host cues. Also peaking at 4.5 ZT are
293 *carbonic anhydrase 12* (Smp_168730), which is a glycoprotein localised on the surface of tegument
294 and contributes to parasite survival and virulence (Da'dara *et al*., 2019), and *Val12* (Smp_123540)
295 which is a putative secreted member of the venom allergen-like family (Chalmers *et al*., 2008).
296 Both are single cell markers for tegumental cell types. *Val12* is a marker for late tegumental
297 progenitor cells ($Sm13^+$ cells)(Wendt *et al*., 2018), and we show it expressed in approximately 500
298 cells that are positioned along the entire length of the male body (**Supplementary figure 7a**).
299 *Val12*$^+$ cells are more abundant dorsally than ventrally, and transcripts reach the body wall
300 musculature, with some extending in the tubercles of the dorsal tegument (**Supplementary figure 7**
301 **b-d**). This *in situ* expression supports protein structural data indicating that it is likely to be
302 secreted/excreted, onto the tegument or into the host environment (Chalmers *et al*., 2008).
303
304 In males two additional day-time networks of interacting genes were predicted. The first was
305 formed of four genes involved in DNA repair (**Supplementary figure 6)**, and the GO term
306 'damaged DNA binding' was significantly enriched (FDR = 0.0036, **Supplementary table 7;**
307 **Supplementary figure 8).** The second included genes putatively involved in ribosome biogenesis
308 (**Supplementary figure 6**); a putative DEAD box ATP-dependent RNA helicase (orthologous to
309 DDX5)(Smp_013790) which cycles with high amplitude (1.4) and is a marker of HES2+ stem cells
310 **(Figure 3),** and a putative AAA family ATPase (Smp_160870) **(Figure 2)** which also exhibits diel
311 expression in females, and whose human ortholog (NVL) regulates 60S ribosomal subunit
312 biogenesis in the nucleolus in a spatiotemporal manner (Nagahama *et al*., 2004).

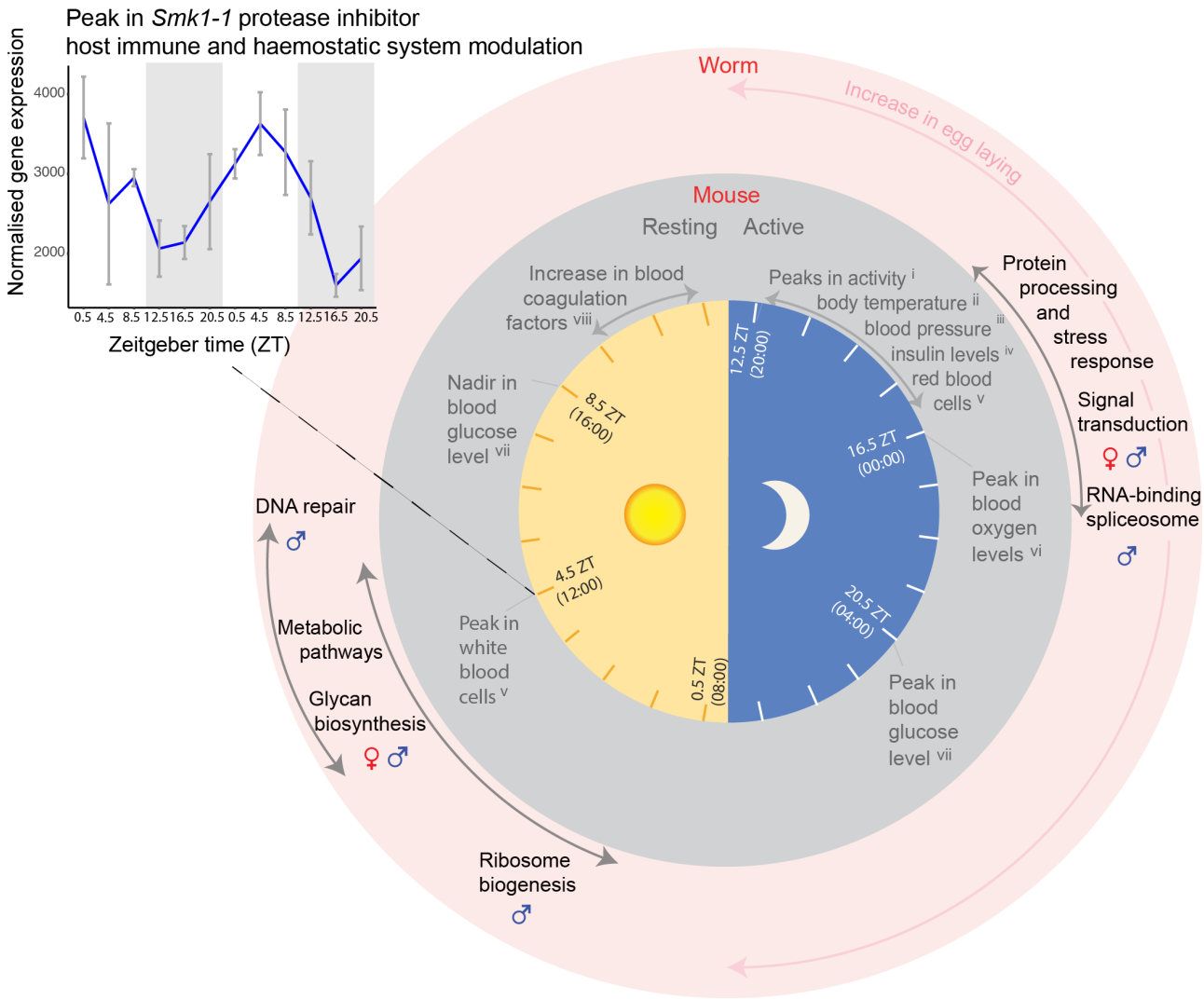

Figure 6. Summary schematic representing the daily rhythms in the transcriptomes of adult *Schistosoma mansoni* (from diel gene enrichment analyses) and the mouse vasculature ([i]Jud *et al*., 2005, [ii]Damiola *et al*., 2004, [iii]Curtis *et al*., 2007, [iv]Feillet *et al*., 2016, [v]Scheiermann *et al*., 2012, [vi]Adamovich *et al*., 2017, [vii]Llanos & de Vacarro, 1972, [viii]Bertolucci *et al*., 2005). Side plot showing temporal expression profile of *Smk1-1*(Smp_307450) in males. Exponentiated, VST-normalised gene expression values are shown, with means taken for each timepoint. Error bars show the standard error of the mean.

The transcriptome patterns associated with the female reproductive system are particularly interesting because schistosome eggs are the cause of disease (including granuloma formation after becoming embedded in the liver and intestine) and transmission. Seventeen of the 21 diel genes that are markers for cell types of the female reproductive system (the vitellarium, germline and Mehlis' gland cells) peak during the day, between 2.5-6.5 ZT. These included a Trematode Eggshell Synthesis domain-containing protein (Smp_326610; Table 1, **Figure 4A**, **Supplementary Table 10**) that is one of several major structural component of the egg shell in schistosomes (Ebersberger *et al*., 2005). Also expressed in phase are other diel genes potentially involved in reproduction (but not identified as cell type markers); a *vasa-like DEAD box ATP-dependent RNA helicase* (Smp_154320, expressed in mature oocytes, *Smvlg2* [Skinner *et al*., 2012]), and a second *putative*

332 *eggshell protein* (Smp_340010). To investigate whether transcriptional rhythms might reveal
333 patterns in egg laying, we recorded day and night egg counts for individual worm pairs *in vitro*. For
334 each of 12 worm pairs, we calculated a day egg count as the median of three consecutive days
335 (three replicates), and a night egg count as the median of three consecutive nights (three replicates).
336 Across the 12 worm pairs, the difference between the night egg count and the corresponding day
337 egg count was significantly higher than zero, that is, paired females tended to lay more eggs at night
338 than during the day (n=12 females; median (night egg count - day egg count) = 12.0; paired
339 Wilcoxon test: P=0.003) (**Figure 4D**). This was also seen in three further independent biological
340 replicates (replicate 2: n=17, paired Wilcoxon test P=0.002, median(night-day)=5.3, replicate 3:
341 n=17, P=0.0003, median(night-day)=17.5; replicate 4: n=8, P=0.008, median(night-day)=14.3)
342 (**Supplementary Figure 9**). Females, on average, laid 13 more eggs over the 12-hour dark phase,
343 corresponding to a 50% increase compared with the light phase.
344
345 3. **Could daily rhythms be generated by a circadian clock intrinsic to *Schistosoma mansoni?***
346 Of the 33 genes that cycle in both sexes, 17 show identical phases and the remaining show
347 acrophases within 4hrs of the opposite sex (**Supplementary figure 10; supplementary Table 4**).
348 These mRNA oscillations in phase between the sexes suggest external cyclical cues drive the
349 synchrony of these rhythms within the *S. mansoni* pairs (and population) inside the mammalian
350 host. Host rhythms may be driving the parasite rhythms, and doing so either directly, or entraining
351 an endogenous time-keeping machinery within the parasite – an intrinsic circadian clock.
352
353 This led us to investigate if *S. mansoni* has homologues of the canonical animal circadian clock
354 genes and whether they show 24-hour periodicity in our datasets. Extensive BLASTP searches
355 revealed that core elements of the negative feedback loop appear to be missing. Even when the
356 stringency was relaxed to an E-value of 1 (BLAST), there were no putative hits for Period or any
357 Cryptochromes (**Supplementary table 11**). We found two DNA photolyases (**Supplementary**
358 **table 12),** which are members of the cryptochrome/photolyase family (CPF), but they clustered
359 with the CPD photolyases, not the canonical animal circadian-related Cryptochromes
360 (**Supplementary figure 11**) and they lacked the FAD binding domain (see **supplementary**
361 **information** for secondary structural features of putative circadian proteins). We identified three
362 bHLH-PAS proteins similar to Clock (Smp_178780 and Smp_168600) and Cycle/Bmal1
363 (Smp_341950)(**Supplementary table 11 & 12**), however phylogenetic analysis showed that they
364 clustered with the closely-related non-circadian proteins ARNT, AHR and SIM (**Supplementary**
365 **figure 11**). Therefore, *S. mansoni* appears to lack the core negative feedback genes, Period and
366 Cryptochromes, as well as the positive transcription factors Clock and Bmal1/Cycle. However, we

367 did identify an orthologue for Timeout (Tim2)(Smp_163340), but not its paralogue Timeless
368 (Tim1) (**Supplementary figure 11, supplementary table 11 & 12**). *Timeout* doesn't cycle in our
369 datasets.
370
371 We identified putative homologs for many secondary clock genes, including orthologs for vrille,
372 slmb/lin23, shaggy/GSK3, and doubletime/Ck1e/KIN-20 (**Supplementary figure 12)**. However,
373 none of the orthologs or other homologues (**Supplementary tables 11 & 12)** have diel expression,
374 even in the male head samples. Although *S. mansoni* orthologs of metazoan clock genes did not
375 show 24-hour periodicity, we found 51 diel genes in *S.mansoni* whose ortholog in another animal
376 also has ~24 hour oscillations in expression (**Supplementary tables 4 & 13)**. *S. mansoni* has 24
377 diel genes in common with *Drosophila melanogaster* (14 genes for male worms, $p = 0.03927$; 15
378 for females, $p = 0.000687$), 32 with mouse (23 for male $p = 0.5179$; 17 for females $p = 0.6248$), and
379 only 4 with another lophotrochozoan, the limpet *Cellana rota* (Schnytzer *et al*., 2018) (4 for
380 females $p = 0.01117$; 2 for males $p = 0.3675$).
381
382 **Discussion**
383 Growing evidence is revealing the importance of biological rhythms in parasites as a strategy to
384 optimize survival within a host and transmission between hosts (Reece *et al*., 2017). Behavioural
385 patterns have been recorded for decades (Westwood *et al*., 2019 and references therein), but only in
386 the last five years, in unicellular parasites, have the underlying molecular oscillations that are
387 responsible for these rhythms been investigated (Rijo-Ferreira *et al*., 2017; Rijo-Ferreira *et al*.,
388 2020). In this study, we have discovered the first 24-hour rhythms in the transcriptomes of a
389 metazoan parasite; revealing that, like free-living animals, the effects of the earth's daily rotation
390 influences the biology of this intravascular flatworm, indirectly, at least. Our study also provides the
391 first insights into biological rhythms of adult *S. mansoni*. We have demonstrated that the
392 transcriptomes of this parasite are not static over the daily cycle, however, the number of diel genes
393 is low compared to other animals; e.g. 5.7% in the water flea, *Daphnia pulex* (Rund *et al*. 2016) and
394 43% of protein coding genes in mouse show circadian rhythms, largely in an organ-specific manner
395 (Zhang *et al*., 2014). We believe there are two reasons for this. First, we pooled six whole animals
396 from a mouse, and sampled three mice at each time point, so any variation in rhythms between host
397 mice, between worms within a pool (from one mouse), and between tissues within each worm,
398 could mask organ-specific oscillations. We expect that many more diel genes will be identified as
399 specific cell types and organs are sampled at this temporal scale, facilitated by recent advances in
400 single cell transcriptomic methods (Wang *et al*., 2018; Wendt *et al*., 2020; Diaz *et al*., 2020).
401 Second, we carried out an initial filtering step to exclude genes from our analysis that were not

402 significantly differentially expressed over a 24 hour period. The JTK_Cycle method alone does not
403 determine whether a transcript varies significantly over time. So this filtering step has reduced false
404 positives, and enabled us to identify diel genes that cycle with high enough amplitudes to be
405 detected in pooled, whole worm samples. The amplitudes of diel genes were also low compared to
406 other animals e.g. median fold change of 2 in *D. pulex* (Rund *et al*. 2016); as diel genes in male
407 head samples had a higher median amplitude than the whole-body samples this suggests that organ-
408 specific cycling might have been dampened in our whole animal samples. The effects of daily
409 oscillations in transcripts has implications for all future RNAseq and functional genomic studies in
410 this species, and the identification of diel genes in this study will allow future experiments to take
411 into account, and control for, the effects of oscillating transcripts.
412
413 We interpreted the daily rhythms in the transcriptomes of *S.mansoni* within the context of what is
414 known about the daily oscillations in mouse vasculature (**Figure 6**). The putative function of
415 *S. mansoni* diel genes and their cell type expression suggest that a number of host daily rhythms
416 may be important zeitgebers to the worms' rhythms; i.e. heat shock triggers, immune and
417 coagulation factors and insulin. The most striking 24-hour rhythm was the nocturnal increase in
418 expression of genes involved in the unfolded protein and stress responses. This revealed
419 rhythmicity in molecular chaperones that are implicated in a wide variety of cellular processes;
420 stabilizing new proteins (Tissières *et al*. 1974), processing proteins damaged by environmental
421 stressors (Rampelt *et al*., 2012), and cell signalling (Stice & Knowlton 2008). Chaperones that have
422 24-hour periodicity in other animals (and are orthologs of *S. mansoni* diel chaperones) are
423 controlled by the circadian clock to regulate protein aggregation and toxicity (Xu *et al*., 2019), and
424 maintain the unfolded protein response (UPR) within a physiologically appropriate range (Eletto *et*
425 *al*., 2014). In *S. mansoni*, increased UPR activity at night might be a response to, or anticipation of,
426 periods of high ER-protein-folding demand that could be triggered by host cyclical rhythms, and
427 this may be an adaptive stress response. One possible trigger is the daily body temperature cycle of
428 the mouse, which increases by up to 4°C as it becomes active and starts feeding at the onset of the
429 dark phase (Damiola *et al*., 2000). Although a relatively moderate increase, this is enough to
430 activate the mouse's own heat shock response (Reinke *et al*., 2008). The daily body temperature
431 cycles of the mouse also drive a rhythmic alternative splicing (AS) program in itself (Preusner *et*
432 *al*., 2017). It is a possibility, therefore, that the increase in the mouse body temperature at night also
433 drives a heat shock response and splicing activity in the worms. Several RNA-binding proteins are
434 involved in splicing regulation in response to heat stress; Ser/Arg-rich splicing factors are known
435 regulators after heat shock (Shin *et al*., 2004), some hnrpH genes have a role in an arrest of mRNA
436 splicing following heat shock (Honore, 2000; Mahe *et al*., 1997), and Hsp70 is known to reactivate

437 mRNA splicing after heat inactivation (Vogel *et al*., 1995). Orthologs of these genes in *S.mansoni*
438 form part of the night-time interaction network in male worms (**Figure 2**). As temperature entrains
439 circadian rhythms in *in vitro* populations of the blood-dwelling unicellular parasite, *Trypanosoma*
440 *brucei* (Rijo-Ferriera *et al*., 2017), it may be an important cyclical cue for *S.mansoni* as well. Other
441 environmental stressors known to activate the heat shock pathway include hypoxia and reactive
442 oxygen species (Kregel, 2002) and as mouse blood oxygen and glucose levels increase during the
443 dark phase (Adamovich *et al*., 2017; Llanos & de Vacarro, 1972), they could also induce the
444 transcription of HSPs in *S. mansoni*. Circumstantial evidence points towards the nocturnal increased
445 expression of heat shock and related genes being involved in proteotoxic stress (and hormone cell
446 signalling) rather than a period of protein synthesis. This is because it is in anti-phase (at the
447 opposite time of day) to rhythmic processes involved in translation regulation and protein synthesis,
448 and it is synchronous with the mouse's active phase and accompanying increases in environmental
449 stressors.
450
451 The most prominent day-time process was a single extended metabolic 'rush hour' that started at
452 the beginning of the hosts resting phase. As feeding can act to gate the initiation of metabolic
453 activities (Sonoda *et al*., 2007) this may indicate a period of nutrient uptake in the worms.
454 *S. mansoni* adults take up glucose and amino acids from the host blood directly across the tegument
455 (Skelly *et al*., 2014), and some diel metabolic genes are markers of tegumental cell types. Worms
456 also ingest blood cells into the digestive system with females thought to feed continuously, and
457 males intermittently (Skelly *et al*., 2014), but there was no evidence of daily rhythms in genes
458 involved in blood cell feeding. Insulin signalling, activated by host insulin, plays an important role
459 in the growth, development and fecundity of schistosomes (Du *et al*., 2017), and is known to
460 influence the maturation of schistosome eggs and their movement into the intestine (You *et al*.,
461 2012; You *et al*., 2015). In mice, blood insulin levels peak at night (Feillet *et al*., 2016, **Figure 6**).
462 In the worms, throughout the night, transcript abundance of genes involved in the insulin signalling
463 pathway increased, and so did egg-laying. It is possible, therefore, that the worms' increase in egg
464 laying rates coincide with periods of higher host insulin levels. However, because this egg-laying
465 experiment was carried out *in vitro*, and therefore in the absence of host cyclical cues, this pattern
466 must be an endogenous rhythm. Host cues, like insulin, however, could act as zeitgebers to
467 synchronise the parasites rhythms to that of its host.
468
469 Although elements of the circadian clock network are conserved across diverse animal lineages
470 (Hardin, 2011; Takahashi, 2017), the more taxa that are investigated the greater the variation
471 discovered (Bell-Pedersen *et al*., 2005; Perrigault & Tran, 2017; Cook *et al*., 2018). A daily

472 program of gene expression clearly exists in *S. mansoni* despite the lack of most of the canonical
473 core clock gene orthologs. This suggests there is either an unusual oscillatory mechanism, or a
474 functional endogenous clock has been lost and the *S. mansoni* rhythms are responding directly to
475 host rhythms. The only core clock gene we found in the genome was Timeout, but it didn't show
476 24-hour periodicity in expression. While its paralog, *Timeless,* functions as a canonical circadian
477 clock gene in *Drosophila* and some other insects (Zheng & Sehgal, 2008; Iwai *et al*., 2006; Zhu *et*
478 *al*., 2008), *Timeout* is a multifunctional gene. Indeed, *Timeout* plays an essential role in the
479 maintenance of chromosome integrity, light entrainment of the circadian clock, embryonic
480 development and regulation of DNA replication (Benna *et al*., 2010; Gotter *et al*., 2000; Gotter *et*
481 *al*., 2007), as well as a role in the mammalian circadian clock (Barnes *et al*., 2003). It has circadian
482 rhythms in the free-living flatworm *Schmidtea mediterranea* (Tsoumtsa *et al*., 2017); and, in female
483 parasitic fig wasps, it only becomes rhythmically expressed once the wasp has successfully
484 dispersed from the dark cavity of the fig, suggesting that rhythmicity is light-dependent (Gu *et al*.,
485 2014). The last common ancestor of the Bilateria is hypothesized to have had all core clock
486 components; Period, Timeless and Timeout, Clock, Cycle/Bmal1 and Cryptochromes (Reitzel *et al*.,
487 2010), and combinations of these are present in extant Lophotrochozoa (Zantke *et al*., 2013;
488 Perrigault & Tran, 2017; Cook *et al*., 2018). This suggests that *S. mansoni* has either lost all but
489 *Timeout*, or these genes have diverged beyond recognition. *S. mansoni* orthologs of secondary clock
490 genes did not show 24-hour periodicity. This could be a sampling artefact due to sequencing RNA
491 from pooled, whole worm samples as clock gene rhythmicity may be limited to a subset of tissues
492 (Whitmore *et al*., 1998), or the phase of clock gene expression can vary between tissues and even
493 between cells within a tissue (Escamilla-Chimal *et al*., 2010; Wen *et al*., 2020). However, even in
494 the male head samples (containing a subset of organs and tissues) there was still no 24-hour cycling
495 of any putative clock gene transcripts. Alternative explanations for lack of 24-hour periodicity
496 could be that they do not have rhythmicity at the transcript level, and/or may have non-clock
497 functions. The adaptive advantage of a clock in environments with neither light nor very high-
498 amplitude environmental cycles is less obvious (Olmedo *et al*., 2012). If, however, in future studies,
499 any of these daily rhythms are discovered to be endogenous circadian rhythms, then our findings
500 suggest that the *S. mansoni* clockwork must be quite distinct from that in other animals, and novel
501 endogenous oscillators may be discovered within our list of diel genes.
502
503 Despite the profound global impact of schistosomiasis, there is complete reliance on only a single
504 drug (praziquantel) for treatment, and evidence of reduced susceptibility in some schistosome
505 populations (Ismail *et al*., 1996; Crellen *et al*., 2016), raises the spectre of drug resistance rendering
506 current control measures ineffective. Consequently, there is a drive to develop a new generation of

507 therapeutics based on schistosome genomes and their function (e.g. Berriman *et al*., 2009; Crosnier
508 *et al*., 2020; Wang *et al*., 2020). Understanding the rhythms of target genes and their products will
509 determine how an organ, or organism, will respond to a drug at a specific time of the day, and the
510 timing of drug delivery could have a large impact on the effectiveness of target activation or
511 inhibition (Cederroth *et al*., 2019). An RNAi screen to uncover new therapeutic targets in
512 *S. mansoni* identified 195 genes that caused parasite detachment and affected survival (Wang *et al*.,
513 2020), eight of which we have identified as diel genes **(Supplementary table 4**), including *Hsp90*
514 (Smp_072330) that demonstrated very high amplitudes in both sexes. By searching the ChEMBL
515 database (Mendez *et al*., 2019), we identified existing drugs that are predicted to target the encoded
516 protein of 26 diel genes, 12 of which are phase IV approved drugs (i.e. with the best safety record
517 for humans), including four metabolic chokepoints (**Supplementary table 14**). The diel genes with
518 the highest amplitudes in each dataset are all putative drug targets, for example *SmKI-1*
519 (Smp_307450) has four phase IV compounds that are predicted to target it, and it is also a proposed
520 vaccine candidate (Hernandez-Goenaga *et al*. 2019). Therefore our fine temporal scale analyses of
521 the *S. mansoni* transcriptomes will provide a useful foundation for the development and delivery of
522 new therapeutics. Although we have described daily rhythms in schistosomes collected from
523 nocturnal mice, we can assume that some of these rhythms will be inverted in worms infecting
524 diurnal humans. The development of new therapeutics against schistosomiasis should include
525 chronobiological information from the parasite and host wherever possible, and investigating
526 further the temporal periods of parasite vulnerability (e.g. the stress response) and metabolic
527 chokepoint activity (during the metabolic rush hour) holds promise for improving human health.
528

529 **Conclusions**

530 Schistosome adults live in the bloodstream of a mammalian host, which is a 24-hour rhythmic
531 environment. Our finding that *S. mansoni* adults have daily rhythms in their transcriptomes is,
532 therefore, not surprising. These daily rhythms in the parasite may be driven by host rhythms, either
533 directly, and/or generated by an intrinsic circadian clock that is entrained to host cues. What is
534 surprising, however, is that exploration of the genome revealed a lack of core clock genes that are
535 generally conserved across other animals, and this is suggestive of an unusual oscillatory
536 mechanism or loss of a functional endogenous clock. Our identification of diel genes and daily
537 processes has revealed fine-scale temporal partitioning of biological processes, some of which may
538 serve the particular time-of-day challenges of life within the host; e.g. a proteotoxic stress response,
539 host immune system modulation and anti-coagulation activity. Future studies will examine how
540 these rhythmic accumulations of mRNA abundance in *S.mansoni*; i) are generated; i.e. the balance

541 between synthesis and degradation; ii) are propagated, i.e. imposed by the host versus endogenously
542 controlled by the parasite itself; and iii) if they eventually exert functions.
543

544 # Methods
545
546 **Ethics statement**
547
548 The life cycle of *Schistosoma mansoni* NMRI (Puerto Rican) strain is maintained at the Wellcome
549 Sanger Institute (WSI) by breeding and infecting susceptible *Biomphalaria glabrata* snails and
550 mice. The procedures involving animals were conducted under the Home Office Project Licence
551 No. P77E8A062 held by GR. All protocols were revised and approved by the Animal Welfare and
552 Ethical Review Body (AWERB) of the WSI. The AWERB is constituted as required by the UK
553 Animals (Scientific Procedures) Act 1986 Amendment Regulations 2012.
554

555 **Animal procedures**
556
557 Female Balb/c mice were bred at the WSI, and maintained on individual air handling units at 19 to
558 23°C and 45–65% humidity. Animals were given access to food and water ad libitum, maintained
559 on a 12-hour light/dark cycle, and housed in groups of no more than 5 adults per cage. Welfare
560 assessments are carried out daily, abnormal signs of behaviour or clinical signs of concern are
561 reported. All personnel at the WSI performing welfare checks on animals are trained and assessed
562 as competent by qualified named individuals.
563

564 Thirty-six 6 weeks old female were percutaneously infected with 200 mixed-sex *Schistosoma*
565 *mansoni* cercariae collected from 13 infected snails as described (Crosnier *et al*., 2019). In brief,
566 under isoflurane anaesthesia, the mice were carefully transferred onto individual holders in a
567 bespoke pre-warmed anaesthesia rig and their tails inserted into the test tubes containing with the
568 cercariae. After 40 minutes exposure, animals are removed from the anaesthesia rigs, placed back
569 into their cage and monitored until full recovery from the anaesthesia. For parasite collection
570 (below) mice were euthanised by intraperitoneal injection of 200 µl of 200 mg/ml pentobarbital
571 (Dolethal®) supplemented with 100 U/ml heparin (cat.# H3393, Sigma Aldrich), and adult worms
572 recovered by portal perfusion (the portal vein is sectioned followed by intracardiac perfusion with
573 phenol-red-free DMEM, cat.# 31053-044 ThermoFisher Scientific, containing 10 U/mL heparin)
574
575 **Parasite collection**
576

577 At 42 days post infection, groups of 3 mice were perfused every 4 hours for 44 hours, and the adult
578 worms collected. The worms sampled in the dark phase were collected from mice euthanized under

579 red light conditions. We collected worm samples 30 minutes after lights on (Zeitgeber time (ZT)
580 0.5) and then 4 hours subsequently giving us collection times of ZT:0.5, 4.5, 8.5, 12.5, 16.5, 20.5
581 over two 24hr periods. ZT:0.5 corresponds to 8am in the human 24hr clock, so actual collection
582 times were 08:00, 12:00, 16:00, 20:00, 00:00, 04:00. At each collection time worms were washed in
583 serum-free DMEM media at 37°C. Mature, paired male and female worms from each mouse were
584 separated and six female worms were pooled and stored in TRIzol at -80°C, and the same for six
585 male worms. A further 10 male worms were pooled from each mouse and fixed and stored in the
586 RNA stabiliser *vivo*PHIX™ (RNAssist Ltd, Cambridge, UK) at 4°C for the dissection of heads the
587 following week. We used male heads only as they are bigger and easier to dissect than female
588 heads. RNA was extracted from each pool and sequenced (**Figure 1A**). From each mouse at each
589 time point, we therefore collected material simultaneously for 3 time-series datasets: pooled
590 females, pooled males and pooled male heads, with 36 samples in male and female datasets, and 33
591 samples of male heads (three perfusions had too few worms to collect for head samples:
592 day1_20:00_b, day2_04:00_b, day2_04:00_c).
593
594 **RNA isolation, library preparation and transcriptome sequencing**
595
596 RNA was isolated from the pooled whole worm samples in TRIzol reagent according to the
597 manufacturer's instructions (Life Technologies). For the male head samples, ten additional male
598 worms per mouse per time point were dissected in *vivo*PHIX™ by cutting posterior to the ventral
599 sucker and anterior to the testes. The heads were rinsed in 50% ethanol and pooled in TRIzol and
600 the RNA extracted as for the whole worm samples. RNA quality was assessed using a Pico RNA kit
601 for the BioAnalyzer (Agilent). We were able to extract good quality RNA from all but one sample
602 (male head day2_20:00_c). Total RNA was enriched for mRNA using poly(A) pulldown. The
603 sequencing libraries were prepared using the NEB Ultra II RNA custom kit on an Agilent Bravo
604 WS automation system. All samples had 14 cycles of PCR, which was set-up using Kapa HiFi Hot
605 start mix and Eurofins dual indexed tag barcodes on Agilent Bravo WS automation system. RNA
606 sequencing of the pooled worm libraries was performed on six lanes of the Illumina HiSeq2500 v4
607 75 Paired End sequencing platform. All sequencing data are available through ENA study accession
608 number ERP108923.
609
610 **Identification of diel cycling transcripts**
611
612 Read quality was assessed using the FASTQC quality control tool. Raw reads were mapped to the
613 *Schistosoma mansoni* genome (version 7, WormBaseParaSite (WBPS version 14, WS271)) using
614 STAR (Dobin, 2013). Genes with fewer than 10 reads mapping across all samples were excluded.

615 Read counts were normalised using DESeq2 v1.22.2 (Love *et al*., 2014) with default parameters
616 and the variance stabilising transformation. Principal Components Analysis was then used to
617 exclude outlier samples by comparing them to replicates. One male sample (day1_12:00_a), two
618 male head samples (day1_20:00_b; day2_20:00_a) and no female samples were excluded.
619
620 To reduce false positive calls of cycling genes, we first excluded genes which were not
621 differentially expressed across the time course using the GLM approach in edgeR v3.24.3
622 (Robinson *et al.,* 2010). Initially only genes with Counts Per Million (CPM) greater than three
623 across at least three samples were included in the analysis. In the model design replicates for
624 equivalent Circadian time in each of the two 24h periods were considered as the same time point.
625 Genes with a False Discovery Rate (FDR) greater than 0.05 were then excluded.
626
627 To identify cycling genes, we used JTK_cycle (Hughes *et al.,* 2010), called using the meta2d
628 function from the MetaCycle software (Wu *et al.,* 2016). Default parameters were used i.e.
629 minimum period 20 hours, maximum period 28 hours. Genes with an FDR < 0.01(JTK BH.Q
630 <0.01) were called as cycling. For visualisation of cycling gene expression, normalised counts for
631 replicates were averaged and then log-transformed to generate heatmaps using the *pheatmap*
632 package with the option scale = 'row'. The fold change of gene expression over the time points
633 was calculated as the max (peak)/ min (trough), keeping replicates separate.
634
635 **Identification of drug targets**
636
637 Drugs from the ChEMBL database that we predict to interact with the cycling genes were identified
638 using the approach described in Wang *et al*. (2020).
639
640 **Gene Ontology enrichment analysis of cycling genes**
641
642 To better understand the function of genes identified as cycling, we performed Gene Ontology (GO)
643 enrichment analysis of our gene lists using topGO (Alexa *et al*., 2006), with FDR < 0.05, node_size
644 = 5, method = 'weight01', statistic = 'Fisher'. GO terms for *S. mansoni* were downloaded from
645 WormBase Parasite using BioMart (Howe *et al*., 2016) on the 5th March 2020.
646
647 **KEGG pathway mapping**
648
649 Mapping of *S. mansoni* gene products to the KEGG pathway database was performed on the KAAS
650 server (https://www.genome.jp/kegg/kaas/) using the GHOSTX program and BBH method. The
651 significance of cycling gene enrichment in pathways was assessed using Fisher's Exact test and

652 resulting P-values were adjusted using the Benjamini-Hochberg procedure, where maps in the
653 KEGG categories 1-4 (https://www.genome.jp/kegg/pathway.html) were tested. Pathways with
654 FDR < 0.05 were considered as significant. For visualisation the R package Pathview (Luo *et al*.,
655 2013) was used.
656
657 **Molecular interactions analysis**
658 Molecular interactions were predicted using the online search tool STRING (www.string-db.org; V
659 11)(Szklarczyk *et al.,* 2015). The *S. mansoni* V7 gene identifiers for diel gene were converted to *S.*
660 *mansoni* V5 gene identifiers. The protein sequences for V5 gene identifiers were analysed in
661 STRINGdb. Protein sequences for day-time peaking genes for each dataset were entered as a
662 multiple protein search. Default settings were used to predict interactions with a minimum
663 interaction (confidence) score of 0.4, corresponding to medium level of confidence. A second
664 identical analysis was carried out for night time peaking genes in male and female worms.
665
666 **Single cell data analysis**
667
668 We used publicly available single cell transcriptome data from mature adult male and female
669 worms (Wendt *et al*., 2020) to determine if cycling transcripts were specific to a certain cell type
670 (i.e. cell type markers), specific to a category of cell types (e.g. muscle, neurons, germline,
671 tegument lineage etc), or more broadly expressed and found in more than one category of cell type.
672 Processed single-cell RNA-seq data were provided by the authors (R object
673 Whole_Integrate_rmv27_50_RN.rds). We used the hypergeometric test to determine whether each
674 cell type cluster contained more marker genes called cycling in our datasets than expected by
675 chance. This was done separately for each of the male, female and male head datasets. The resulting
676 p-values were corrected using the Benjamini-Hochberg method. A Python script implementing this
677 method is available from our GitHub page
678 (https://github.com/adamjamesreid/schistosoma_daily_rhythms/).
679
680 Seurat UMAP plots were used to explore the expression of cycling transcripts across cell types and
681 whether they were ubiquitously expressed or enriched, or specific, to one or more cell type (Stuart
682 *et al*., 2019). Some of the cycling transcripts identified as cell type markers and enriched in specific
683 cell types were validated by *in situ* hybridization (below).
684
685 **Identification of hypothetical proteins**
686

687 Amino acid sequences for the ten diel hypothetical proteins were obtained from WormBaseParasite.
688 Protein 3D structures were predicted from amino acid sequences using I-TASSER online
689 server(v5.0) (Yang *et al.,* 2015) with default parameters. TM-scores indicate similarity between two
690 structures. The values range from 0-1, with the value of 1 indicating a perfect match.
691
692 ***Fluorescent in situ* hybridisation and imaging**
693
694 Mature adult pairs, collected from mice infected for life cycle maintenance and parasite material
695 production, were anaesthetised in 0.5% solution of ethyl 3-aminobenzoate methanesulfonate
696 (Sigma-Aldrich, St. Louis, MO) for 15 minutes to separate male and female worms. The worms
697 were killed in 0.6 M MgCl2 for 1 min, and incubated in 4% formaldehyde in PBSTx (1xPBS +
698 0.3% TritonX) for 4 hours at room temperature. They were rinsed 3 x 5minutes in PBSTx,
699 dehydrated into 100% Methanol and stored at -20C. Samples were gradually rehydrated in PBSTx
700 over 30minutes and incubated in 5ug/ml Proteinase K (Invitrogen) in 1x PBSTx for 30 minutes at
701 37°C. They were post-fixed in 4% Formaldehyde in PBSTx for 10 min at room temperature then
702 rinsed in PBSTx for 10 minutes. Probes, buffers, and hairpins for third generation *in situ*
703 hybridization chain reaction (HCR) experiments were purchased from Molecular Instruments (Los
704 Angeles, California, USA). Experiments were performed following the protocol described by Choi
705 *et al*. (2016; 2018) and developed for wholemount nematode larvae. Samples were mounted using
706 DAPI fluoromount-G (Southern Biotech) and imaged on a confocal laser microscope (Sp8 Leica).
707
708 ***In vitro* egg laying assay**
709 Twelve freshly perfused pairs of adult worms (still coupled) were placed into individual wells of a
710 12-well plate containing 3 ml of ABC169 media (Wang *et al*., 2019) and kept at 37°C, 5%CO_2 in
711 the dark. Eggs from each well were collected, and counted, at 8am and 8pm every day for 72 hours,
712 giving 3 day-time counts and 3 night-time counts per worm couple. The first 12 hour period post-
713 perfusion was discounted to allow the worms to acclimate to the *in vitro* conditions. This
714 experiment was replicated 3 times, each time with freshly perfused worms. The median egg number
715 for each worm for day-time, and night-time was calculated and a paired Wilcoxon test was carried
716 out to determine if there was a significant difference in the number of eggs laid between day or
717 night.
718
719 **Identification of core, and secondary, circadian clock genes in *Schistosoma mansoni***
720
721 We identified putative *Schistosoma mansoni* homologues of animal circadian clock genes using two
722 methodologies. The first was a BLASTP sequence similarity search with a cut off e-value of 1e-10

723 against the *S. mansoni* genome (v7) in WormBaseParaSite (WBPS version 14, WS271), using
724 previously defined circadian proteins sequences from UniProtKB (Boutet *et al.*2007) and GenBank
725 (**Supplementary Table 9**). Our second method enhanced the robustness of our searches by using
726 respective domains of proteins to identify putative orthologues, as shown before (Padalino *et al.*
727 2018). Briefly, domain identifiers for main clock proteins were selected using Pfam and SMART,
728 and their respective signatures were used to query the BioMart function in WBPS against the entire
729 *S. mansoni* genome (**Supplementary Table 10**). A BLASTP of output sequences in NCBI
730 (Altschul *et al.*1990) was used to identify these proteins, and all respective hits were aligned in
731 Jalview 2 and illustrated in IBS illustrator (Liu *et al*. 2015).
732
733 To examine whether hits were orthologous to circadian clock proteins from other animals,
734 phylogenetic analyses on the core clock components were conducted; Timeless/Timeout,
735 Cycle/BMAL1/Arntl and Clock (all are basic helix-loop-helix-PAS proteins) and the
736 Cryptochromes/ Photolyases, and the secondary clock proteins; Vrille, Slmb, Shaggy and
737 Doubletime. Sequences were aligned using CLUSTAL OMEGA (Sievers *et al*. 2011) and visually
738 examined using Jalview 2 (Waterhouse *et al*. 2009). The aligned sequences were exported into
739 Gblocks 0.91b (Castresana, 2000) with allowance for smaller blocks and less strict flanking
740 positions for reduced stringency. Conserved positions (3% for bHLH/PAS, 9% for CDP photolyase,
741 16% for timeless) were used to construct a Neighbour-Joining phylogenetic tree (JTT model) with
742 partial/pairwise deletion and 1000 bootstrap replications in MEGA-X (Kumar *et al*. 2018).
743
744 **Comparison of diel 1-to-1 orthologs in *Schistosoma mansoni* and other Metazoa**
745
746 We identified 2925 cycling genes in *Drosophila melanogaster* from the Cycling Gene Data Base
747 (CGDB; Li *et al*., 2017) and 3233 *S. mansoni-D. melanogaster* one-to-one orthologues from
748 Wormbase Parasite (Bolt *et al*., 2018). Of the one-to-one orthologues, 420 cycled in *D.*
749 *melanogaster*, 66 in *S. mansoni* males, 48 in females. For mouse, we identified 9534 cycling genes
750 from CGDB and 2855 one-to-one orthologues with *S. mansoni* using Wormbase Parasite. 1146
751 shared orthologues were cycling in mouse, 57 in male, 44 in female. To examine common cycling
752 genes between *S. mansoni* and another lophotrochozoan, we used the 221 cycling limpet (*Cellana*
753 *rota*) transcripts identified by Schnytzer *et al*. (2018). A total of 38,482 limpet translated transcript
754 sequences were used with 14499 sequences from *S. mansoni* (WBPS15) to identify one-to-one
755 orthologues using OrthoFinder (Emms & Kelly, 2019). Here we looked for shared orthogroups
756 rather than one-to-one orthologues due to the fragmented nature of the limpet transcriptome
757 assembly. There were 5025 shared orthogroups between limpet and *S. mansoni*. 67 limpet cyclers
758 and 96 *S. mansoni* cyclers were in shared orthogroups. We used the Fisher exact test to determine

759 whether the number of one-to-one orthologues cycling in both species was greater than expected by
760 chance.
761

762 **Acknowledgements**
763

764 We thank all members of the Parasite Genomics team at the Wellcome Sanger Institute for their
765 comments and input on this study. We thank the animal facility staff – Simon Clare and his team,
766 and David Goulding of the Electron and Advanced Light Microscope Facility for their support &
767 assistance in this work. We thank Andrew Goldsborough of RNAssist Ltd for advice on RNA
768 stabilisation and Anna Protasio for discussion on RNA sequencing. We thank Jim Collins and his
769 lab for helpful discussion on their single cell data. The infrastructure used for this analysis is
770 maintained by the core IT Service and the Pathogen Informatics teams at Wellcome Sanger
771 Institute. The research was supported by a Wellcome Trust Janet Thornton Fellowship (WT206194)
772 to KR.
773
774

775 **Competing interests**
776

777 The authors declare that no competing interests exist.
778

779 **References**
780

781 Adamovich Y, Ladeuix B, Golik M, Koeners MP, Asher G (2017) Rhythmic oxygen levels reset
782 circadian clocks through HIF1alpha. Cell Metab. 25 93–101. doi:10.1016/j.cmet.2016.09.014
783

784 Alexa A, Rahnenführer J, Lengauer T (2006) Improved scoring of functional groups from gene
785 expression data by decorrelating GO graph structure. Bioinformatics 22:1600-7.
786 doi:10.1093/bioinformatics/btl140.
787

788 Altschul SF, Gish W, Miller W, Myers EW, Lipman DJ (1990) Basic local alignment search tool.
789 Journal of Molecular Biology. 215:403-410. doi:10.1016/S0022-2836(05)80360-2.
790

791 Ash C, Dubec M, Donne K, Bashford T (2017) Effect of wavelength and beam width on penetration
792 in light-tissue interaction using computational methods. Lasers Med Sci 32:1909-1918.
793 doi:10.1007/s10103-017-2317-4.
794

795 Barnes JW, Tischkau SA, Barnes JA, Mitchell JW, Burgoon PW, Hickok JR, Gillette MU. (2003)
796 Requirement of mammalian Timeless for circadian rhythmicity. Science. 302 (5644): 439-42.
797 doi:10.1126/science.1086593.
798

799 Benna C, Bonaccorsi S, Wülbeck C, Helfrich-Förster C, Gatti M, Kyriacou CP, Costa R, Sandrelli
800 F (2010) *Drosophila* timeless2 is required for chromosome stability and circadian photoreception.
801 Curr Biol. 23;20(4):346-52. doi:10.1016/j.cub.2009.12.048.
802

803 Berriman M, Haas BJ, LoVerde PT, Wilson RA, Dillon GP, Cerqueira GC, Mashiyama ST, Al-
804 Lazikani B, Andrade LF, Ashton PD, Aslett MA, Bartholomeu DC, Blandin G, Caffrey CR,
805 Coghlan A, Coulson R, Day TA, Delcher A, DeMarco R, Djikeng A, Eyre T, Gamble JA, Ghedin
806 E, Gu Y, Hertz-Fowler C, Hirai H, Hirai Y, Houston R, Ivens A, Johnston DA, Lacerda D, Macedo
807 CD, McVeigh P, Ning Z, Oliveira G, Overington JP, Parkhill J, Pertea M, Pierce RJ, Protasio AV,
808 Quail MA, Rajandream MA, Rogers J, Sajid M, Salzberg SL, Stanke M, Tivey AR, White O,
809 Williams DL, Wortman J, Wu W, Zamanian M, Zerlotini A, Fraser-Liggett CM, Barrell BG, El-

Sayed NM. (2009) The genome of the blood fluke *Schistosoma mansoni*. Nature 16;460 (7253):352-8. doi:10.1038/nature08160.

Bolt BJ, Rodgers FH, Shafie M, Kersey PJ, Berriman M, Howe KL. Using WormBase ParaSite: An Integrated Platform for Exploring Helminth Genomic Data. Methods Mol Biol. 2018;1757:471-491. doi: 10.1007/978-1-4939-7737-6_15. PMID: 29761467.

Boutet E, Lieberherr D, Tognolli M, Schneider M, Bairoch A. (2007) UniProtKB/Swiss-Prot. Methods Mol Biol. 406:89-112. doi: 10.1007/978-1-59745-535-0_4.

Bell-Pedersen D, Cassone VM, Earnest DJ, Golden SS, Hardin PE, Thomas TL, Zoran MJ. Circadian rhythms from multiple oscillators: lessons from diverse organisms. Nat Rev Genet. 2005 Jul;6(7):544-56. doi: 10.1038/nrg1633. PMID: 15951747; PMCID: PMC2735866.

Bertolucci C, Pinotti M, Colognesi I. Foà A, Bernardi F, Portaluppi F (2005) Circadian rhythms in mouse blood coagulation. J Bio Rhythms, 20, 219-224. doi:10.1177/0748730405275654

Catalano S, Sène M, Diouf ND, Fall CB, Borlase A, Léger E, Bâ K, Webster JP (2018) Rodents as Natural Hosts of Zoonotic *Schistosoma* Species and Hybrids: An Epidemiological and Evolutionary Perspective From West Africa, *The Journal of Infectious Diseases*, Volume 218, Issue 3, 429–433, https://doi.org/10.1093/infdis/jiy029

Castresana J (2000) Selection of conserved blocks from multiple alignments for their use in phylogenetic analysis. Mol Biol Evol. 17(4):540-52.

Cederroth CR, Albrecht U, Bass J, Brown SA, Dyhrfjeld-Johnsen J, Gachon F, Green CB, Hastings MH, Helfrich-Förster C, Hogenesch JB, Lévi F, Loudon A, Lundkvist GB, Meijer JH, Rosbash M, Takahashi JS, Young M, Canlon B (2019) Medicine in the fourth dimension Cell Metab 30:238-250 doi:10.1016/j.cmet2019.06.019

Chalmers, I.W., McArdle, A.J., Coulson, R.M. *et al.* Developmentally regulated expression, alternative splicing and distinct sub-groupings in members of the *Schistosoma mansoni* venom allergen-like (SmVAL) gene family. *BMC Genomics* 9, 89 (2008). https://doi.org/10.1186/1471-2164-9-89

Cheung-Flynn J, Prapapanich V, Cox MB, Riggs DL, Suarez-Quian C, Smith DF (2005) Physiological role for the cochaperone FKBP52 in androgen receptor signalling. Mol Endocrinol. 19:1654-66. doi: 10.1210/me.2005-0071.

Choi HMT, Calvert CR, Husain N, Huss D, Barsi JC, Deverman BE, Hunter RC, Kato M, Lee SM, Abelin ACT, et al. (2016). Mapping a multiplexed zoo of mRNA expression. Development 143, 3632-3637. doi:10.1242/dev.140137

Choi HMT, Schwarzkopf M, Fornace ME, Acharya A, Artavanis G, Stegmaier J, Cunha A, Pierce NA (2018) Third-generation *in situ* hybridization chain reaction: multiplexed, quantitative, sensitive, versatile, robust. Development 145: dev165753 doi: 10.1242/dev.165753

Cook GM, Gruen AE, Morris J, Pankey MS, Senatore A, Katz PS, Watson WH 3rd, Newcomb JM (2018) Sequences of circadian clock proteins in the Nudibranch Molluscs *Hermissenda crassicornis*, *Melibe leonina*, and *Tritonia diomedea*. Biol Bull. 234(3):207-218. doi: 10.1086/698467.

857 Crellen T, Walker M, Lamberton PH, Kabatereine NB, Tukahebwa EM, Cotton JA, Webster JP
858 (2016) Reduced efficacy of praziquantel against *Schistosoma mansoni* is associated with multiple
859 rounds of mass drug administration. Clin Infect Dis. 63(9):1151-1159. doi: 10.1093/cid/ciw506.
860
861 Crosnier C, Brandt C, Rinaldi G McCarthy C, Barker C, Clare S, Berriman M, Wright GJ
862 (2019) Systematic screening of 96 *Schistosoma mansoni* cell-surface and secreted antigens does not
863 identify any strongly protective vaccine candidates in a mouse model of infection. Wellcome Open
864 Research, 4:159 doi.org/10.12688/wellcomeopenres.15487.1
865
866 Crosnier C, Hokke CH, Protasio AV, Brandt C, Rinaldi G, Langenberg MCC, Clare S, Janse JJ,
867 Shona Wilson, Matthew Berriman, Meta Roestenberg, Gavin J Wright (2020) Screening of a library
868 of recombinant *Schistosoma mansoni* proteins with sera from murine and human controlled
869 infections identifies early serological markers, *The Journal of Infectious Diseases*
870 doi.org/10.1093/infdis/jiaa329
871
872 Curtis AM, Cheng Y, Kapoor S, Reilly D, Price TS, FitzFerald GA (2007) Circadian variation of
873 blood pressure and the vascular response to asynchronous stress. PNAS 104:3450-3455.
874 doi.org/10.1073/pnas.0611680104
875
876 Da'dara AA, Angeli A, Ferraroni M, Supuran CT, Skelly PJ. Crystal structure and chemical
877 inhibition of essential schistosome host-interactive virulence factor carbonic anhydrase
878 SmCA. *Commun Biol*. 2019;2:333. Published 2019 Sep 5. doi:10.1038/s42003-019-0578-0
879
880 Damiola F., Le Minh N., Preitner N., Kornmann B., Fleury-Olela F., Schibler U. (2000) Restricted
881 feeding uncouples circadian oscillators in peripheral tissues from the central pacemaker in the
882 suprachiasmatic nucleus. Genes & Dev. 14:2950–2961.
883
884 De Filippo K, Rankin SM. (2018) CXCR4, the master regulator of neutrophil trafficking in
885 homeostasis and disease. Eur J Clin Invest.48 Suppl 2; e12949. doi: 10.1111/eci.12949.
886
887 Diaz Soria, C.L., Lee, J., Chong, T. Tracey A, Young MD, Andrews T, Hall Cm Ng BL, Rawlinson
888 K, Doyle SR, Leonard S, Lu Z, Bennett HM, Rinaldi G, Newmark PA, Berriman M (2020) Single-
889 cell atlas of the first intra-mammalian developmental stage of the human parasite *Schistosoma*
890 *mansoni*. Nat Commun 11, 6411 (2020). https://doi.org/10.1038/s41467-020-20092-5
891
892 Dobin A, Davis CA, Schlesinger F, Drenkow J, Zaleski C, Jha S, Batut P, Chaisson M, Gingeras
893 TR (2013) STAR: ultrafast universal RNA-seq aligner, Bioinformatics 29: 15–21.
894 https://doi.org/10.1093/bioinformatics/bts635
895
896 Du, X., McManus, D.P., Cai, P. et al.(2017) Identification and functional characterisation of a
897 Schistosoma japonicum insulin-like peptide. Parasites Vectors 10, 181.
898 https://doi.org/10.1186/s13071-017-2095-7
899
900 Ebersberger, I., Knobloch, J. & Kunz, W. (2005) Cracks in the shell—zooming in on eggshell
901 formation in the human parasite *Schistosoma mansoni*. Dev Genes Evol 215, 261–267.
902 https://doi.org/10.1007/s00427-005-0467-z
903
904 Eletto D, Eletto D, Dersh D, Gidalevitz T, Argon Y. Protein disulfide isomerase A6 controls the
905 decay of IRE1α signaling via disulfide-dependent association. Mol Cell. 2014 Feb 20;53(4):562-
906 576. doi: 10.1016/j.molcel.2014.01.004. Epub 2014 Feb 6. PMID: 24508390; PMCID:
907 PMC3977204.
908

909 Emms DM, Kelly S. OrthoFinder: phylogenetic orthology inference for comparative genomics.
910 Genome Biol. 2019 Nov 14;20(1):238. doi: 10.1186/s13059-019-1832-y. PMID: 31727128;
911 PMCID: PMC6857279.
912
913 Escamilla-Chimal EG, Velázquez-Amado RM, Fiordelisio T, Fanjul-Moles ML. (2010) Putative
914 pacemakers of crayfish show clock proteins interlocked with circadian oscillations. J Exp Biol.
915 213(Pt 21):3723-33. doi: 10.1242/jeb.047548.
916
917 Feillet C, Guérin S, Lonchampt M, Dacquet C, Gustafsson JA, Delaunay F, Teboul (2016) Sexual
918 dimorphism in circadian physiology is altered in LXRα deficient mice. PLoS ONE 11(3):
919 e0150665. doi:10.1371/journal.pone.0150665

920 Global Burden of Disease Study 2019 (GBD 2019) Results [Global Burden of Disease
921 Collaborative Network] *Institute for Health Metrics and Evaluation (IHME)*
922
923 Gotter AL, Manganaro T, Weaver DR, Kolakowski LF Jr, Possidente B, Sriram S, MacLaughlin
924 DT, Reppert SM. (2000) A time-less function for mouse timeless. Nat Neurosci. 3(8):755-6. doi:
925 10.1038/77653.
926
927 Gotter AL, Suppa C, Emanuel BS. (2007) Mammalian TIMELESS and Tipin are evolutionarily
928 conserved replication fork-associated factors. J Mol Biol. 9;366(1):36-52. doi:
929 10.1016/j.jmb.2006.10.097.
930
931 Grover P, Asa, JS, Campos EI (2018) H3-H4 Histone Chaperone Pathways. Annu. Rev. Genet.52:
932 109-130 doi: 10.1146/annurev-genet-120417-031547
933
934 Gu HF, Xiao JH, Niu LM, Wang B, Ma GC, Dunn DW, Huang DW. (2014) Adaptive evolution of
935 the circadian gene timeout in insects. Sci Rep. 4:4212. doi: 10.1038/srep04212.
936
937 Hardin PE. (2011) Molecular genetic analysis of circadian timekeeping in *Drosophila*. *Adv. Genet.*
938 74, 141–173. doi.org/10.1016/B978-0-12-387690-4.00005-2
939
940 Harris AR, Russell RJ, Charters AD. A review of schistosomiasis in immigrants in Western
941 Australia, demonstrating the unusual longevity of Schistosoma mansoni. Trans R Soc Trop Med
942 Hyg. 1984;78(3):385-8. doi: 10.1016/0035-9203(84)90129-9. PMID: 6464135.
943
944 Hernández-Goenaga J, López-Abán J, Protasio AV, Vicente Santiago B, Del Olmo E, Vanegas M,
945 Fernández-Soto P, Patarroyo MA, Muro A. (2019) Peptides derived of kunitz-type serine protease
946 inhibitor as potential vaccine against experimental Schistosomiasis. Front Immunol. 10:2498. doi:
947 10.3389/fimmu.2019.02498.
948
949 Honoré B. (2000) The hnRNP 2H9 gene, which is involved in the splicing reaction, is a multiply
950 spliced gene. Biochim Biophys Acta. 1492(1):108-19. doi: 10.1016/s0167-4781(00)00092-0.
951
952 Howe KL, Bolt BJ, Shafie M, Kersey P, Berriman M (2016) WormBase ParaSite - a comprehensive
953 resource for helminth genomics. Mol Biochem Parasitol 215:2-10.doi:
954 10.1016/j.molbiopara.2016.11.005.
955
956 Hughes ME, Hogenesch JB, Kornacker K (2010) JTK_CYCLE: an efficient nonparametric
957 algorithm for detecting rhythmic components in genome-scale data sets J Biol Rhythms 25:372-
958 80. doi: 10.1177/0748730410379711.
959

International Helminth Genomes Consortium., Coghlan, A., Tyagi, R. et al. (2019) Comparative genomics of the major parasitic worms. Nat Genet 51, 163–174. https://doi.org/10.1038/s41588-018-0262-1

Ismail M, Metwally A, Farghaly A, Bruce J, Tao LF, Bennett JL (1996) Characterization of isolates of *Schistosoma mansoni* from Egyptian villagers that tolerate high doses of praziquantel. American Journal of Tropical Medicine and Hygiene. 1996;55:214–218

Iwai S, Fukui Y, Fujiwara Y, Takeda M. (2006) Structure and expressions of two circadian clock genes, period and timeless in the commercial silkmoth, Bombyx mori. J Insect Physiol. 52(6):625-37. doi: 10.1016/j.jinsphys.2006.03.001.

Jud C, Schmutz I, Hampp G. Oster H, Albrecht U (2005) A guideline for analyzing circadian wheel-running behavior in rodents under different lighting conditions. *Biol. Proced. Online* 7:101–116. doi.org/10.1251/bpo109

Kregel KC. (2002) Molecular biology of thermoregulation: invited review: Heat shock proteins: modifying factors in physiological stress responses and acquired thermotolerance. J. Appl. Physiol. 92:2177–86.

Kumar S, Stecher G, Li M, Knyaz C, Tamura K. (2018) MEGA X: molecular evolutionary genetics analysis across computing platforms. Mol Biol Evol.35(6):1547-9.

Llanos JM, Epele de Vaccaro ME (1972) Circadian rhythm in blood glucose levels in normal and hepatectomized mice, Biological Rhythm Research, 3:1, 25-32, DOI: 10.1080/09291017209359294

Li H, Wang Z, Zhou X, Cheng Y, Xie Z, Manley JL, Feng Y. (2013) Far upstream element-binding protein 1 and RNA secondary structure both mediate second-step splicing repression. Proc Natl Acad Sci U S A.110(29):E2687-95. doi: 10.1073/pnas.1310607110.

Li S, Shui K, Zhang Y, Lv Y, Deng W, Ullah S, Zhang L, Xue Y. CGDB: a database of circadian genes in eukaryotes. Nucleic Acids Res. 2017 Jan 4;45(D1):D397-D403. doi: 10.1093/nar/gkw1028. PMID: 27789706; PMCID: PMC5210527.

Liu W, Xie Y, Ma J, Luo X, Nie P, Zuo Z, Lahrmann U, Zhao Q, Zheng Y, Zhao Y, Xue Y, Ren J. (2015) IBS: an illustrator for the presentation and visualization of biological sequences. Bioinformatics. 31:3359-61. doi: 10.1093/bioinformatics/btv362.

Love MI, Huber W, Anders S (2014) Moderated estimation of fold change and dispersion for RNA-seq data with DESeq2. Genome Biol 15(12):550. doi: 10.1186/s13059-014-0550-8.

Luo W, Brouwer C. (2013) Pathview: an R/Bioconductor package for pathway-based data integration and visualization. Bioinformatics. 15;29(14):1830-1. doi: 10.1093/bioinformatics/btt285.

Mahe D, Mahl P, Gattoni R, Fischer N, Mattei MG, et al. (1997) Cloning of human 2H9 heterogeneous nuclear ribonucleoproteins. Relation with splicing and early heat shock-induced splicing arrest. J Biol Chem 272: 1827–1836.

Maze I, Wenderski W, Noh KM, Bagot RC, Tzavaras N, Purushothaman I, Elsässer SJ, Yin G, Ionete C, Hurd YL, Tamminga CA, Halene T, Farrelly L, Soshnev AA, Wen D, Rafii S, Birtwistle

1012 MR, Akbarian S, Buchholz BA, Blitzer RD, Nestler EJ, Yuan ZF, Garcia BA, Shen L, Molina H,
1013 Allis CD (2015) Critical Role of Histone Turnover in Neuronal Transcription and Plasticity. Neuron
1014 87(1):77-94. doi: 10.1016/j.neuron.2015.06.014.
1015
1016 Mebius MM, van Genderen PJJ, Urbanus RT, Tielens AGM, de Groot PG, van Hellemond JJ
1017 (2013) Interference with the Host Haemostatic System by Schistosomes. PLoS Pathog 9(12):
1018 e1003781. doi.org/10.1371/journal.ppat.1003781
1019
1020 Mendez D, Gaulton A, Bento AP, Chambers J, De Veij M, Félix E, Magariños MP, Mosquera JF,
1021 Mutowo P, Nowotka M, Gordillo-Marañón M, Hunter F, Junco L, Mugumbate G, Rodriguez-Lopez
1022 M, Atkinson F, Bosc N, Radoux CJ, Segura-Cabrera A, Hersey A, Leach AR. (2019) ChEMBL:
1023 towards direct deposition of bioassay data. Nucleic Acids Res. Jan 8;47(D1):D930-D940. doi:
1024 10.1093/nar/gky1075.
1025
1026 Mickum ML, Prasanphanich NS, Heimburg-Molinaro J, Leon KE, Cummings RD (2014)
1027 Deciphering the glycogenome of schistosomes. Front. Genet. 5:262
1028 doi.org/10.3389/fgene.2014.0026
1029
1030 Morais SB, Figueiredo BC, Assis NRG, Homan J, Mambelli FS, Bicalho RM, Souza C, Martins
1031 VP, Pinheiro CS, Oliveira SC (2018) *Schistosoma mansoni Sm*KI-1 or its c-terminal fragment
1032 induces partial protection against *S. mansoni* infection in Mice. Front Immunol. 9: 1762.
1033 doi:10.3389/fimmu.2018.01762
1034
1035 Mouahid G, Idris MA, Verneau O, Théron A, Shaban MMA, Moné H (2012) A new chronotype of
1036 Schistosoma mansoni: adaptive significance. Tropical Medicine and International Health. 17:727-
1037 732
1038
1039 Nagahama M, Hara Y, Seki A, Yamazoe T, Kawate Y, Shinohara T, Hatsuzawa K, Tani K, Tagaya
1040 M. (2004) NVL2 is a nucleolar AAA-ATPase that interacts with ribosomal protein L5 through its
1041 nucleolar localization sequence. Mol Biol Cell. 15(12):5712-23. doi: 10.1091/mbc.e04-08-0692.
1042
1043 O'Donnell AJ, Schneider P, McWatters HG, Reece SE (2011) Fitness costs of disrupting circadian
1044 rhythms in malaria parasites Proc. R. Soc. B.278 2429–2436
1045 https://doi.org/10.1098/rspb.2010.2457
1046
1047 Olmedo M, O'Neill JS, Edgar RS, Valekunja UK, Reddy AB, Merrow M. (2012) Circadian
1048 regulation of olfaction and an evolutionarily conserved, nontranscriptional marker in
1049 Caenorhabditis elegans. Proc Natl Acad Sci U S A.109(50):20479-84. doi:
1050 10.1073/pnas.1211705109.
1051
1052 Padalino G, Ferla S, Brancale A, Chalmers IW, Hoffmann KF (2018) Combining bioinformatics,
1053 cheminformatics, functional genomics and whole organism approaches for identifying epigenetic
1054 drug targets in *Schistosoma mansoni*, International Journal for Parasitology: Drugs and Drug
1055 Resistance. 8:559-570. doi.org/10.1016/j.ijpddr.2018.10.005.
1056
1057 Perrigault M, Tran D. (2017) Identification of the Molecular Clockwork of the Oyster Crassostrea
1058 gigas. PLoS One. 12(1):e0169790. doi: 10.1371/journal.pone.0169790.
1059
1060 Preußner M, Goldammer G, Neumann A, Haltenhof T, Rautenstrauch P, Müller-McNicoll M, Heyd
1061 F. (2017) Body Temperature Cycles Control Rhythmic Alternative Splicing in Mammals. Mol Cell.
1062 67(3):433-446.e4. doi: 10.1016/j.molcel.2017.06.006.
1063

1064 Rampelt H, Kirstein-Miles J, Nillegoda NB, Chi K, Scholz SR, Morimoto RI, Bukau B. (2012).
1065 Metazoan Hsp70 machines use Hsp110 to power protein disaggregation. EMBO J. 31, 4221–4235.
1066 (10.1038/emboj.2012.264)
1067
1068 Ranasinghe SL, Fischer K, Gobert GN, McManus DP (2015) Functional expression of a novel
1069 Kunitz type protease inhibitor from the human blood fluke *Schistosoma mansoni*. Parasites &
1070 Vectors 8: 408 doi.org/10.1186/s13071-015-1022-z
1071
1072 Reece SE, Prior KF, Mideo N (2017) The life and times of parasites: rhythms in strategies for
1073 within-host survival and between-host transmission. Journal of Biological Rhythms, 32(6):516-33.
1074 https://doi.org/10.1177%2F0748730417718904
1075
1076 Reinke H, Saini C, Fleury-Olela F, Dibner C, Benjamin IJ, Schibler U. (2008) Differential display
1077 of DNA-binding proteins reveals heat-shock factor 1 as a circadian transcription factor. Genes Dev.
1078 22(3):331-45. doi: 10.1101/gad.453808.
1079
1080 Reitzel AM, Behrendt L, Tarrant AM. (2010) Light entrained rhythmic gene expression in the sea
1081 anemone *Nematostella vectensis*: the evolution of the animal circadian clock. PLoS One.
1082 5(9):e12805. doi: 10.1371/journal.pone.0012805.
1083
1084 Rijo-Ferreira F, Pinto-Neves D, Barbosa-Morais NL, Takahashi JS, Figueiredo LM (2017)
1085 *Trypanosoma brucei* metabolism is under circadian control. *Nat. Microbiol.* 2, 17032.
1086
1087 Rijo-Ferreira F, Acosta-Rodriguez VA, Abel JH, Kornblum I, Bento I, Kilaru G, Klerman EB,
1088 Mota MM, Takahashi JS (2020) The malaria parasite has an intrinsic clock *Science* 368, 746-753
1089 DOI: 10.1126/science.aba2658
1090
1091 Robinson MD, McCarthy DJ, Smyth GK (2010) edgeR: a Bioconductor package for differential
1092 expression analysis of digital gene expression data. Bioinformatics;26(1):139-40. doi:
1093 10.1093/bioinformatics/btp616
1094
1095 Rund SSC, Yoo B, Alam C, Green T, Stephens MT, Zeng E, George GF, Sheppard AD, Duffield
1096 GE, Milenković T, Pfrender ME (2016). Genome-wide profiling of 24 hr diel rhythmicity in the
1097 water flea, *Daphnia pulex:* network analysis reveals rhythmic gene expression and enhances
1098 functional gene annotation. *BMC Genomics* 17, 653 (2016). https://doi.org/10.1186/s12864-016-
1099 2998-2
1100
1101 Scheiermann C, Kunisaki Y, Lucas D, Chow A, Jang JE, Zhang D, Hashimoto D, Merad M,
1102 Frenette PS (2012) Adrenergic nerves govern circadian leukocyte recruitment to tissues. Immunity
1103 37:290–301 doi.org/10.1016/j.immuni.2012.05.021
1104
1105 Schnytzer Y, Simon-Blecher N, Li J,Waldman Ben-Asher H, Salmon-Divon M,
1106 Achituv Y, Hughes ME, Levy O (2018) Tidal and diel orchestration of behaviour and gene
1107 expression in an intertidal mollusc. Scientific Reports 8: 4917
1108
1109 Shin, C., Feng, Y. & Manley, J. (2004) Dephosphorylated SRp38 acts as a splicing repressor in
1110 response to heat shock. Nature 427, 553–558. doi.org/10.1038/nature02288
1111
1112 Sievers F, Wilm A, Dineen D, Gibson TJ, Karplus K, Li W, Lopez R, McWilliam H, Remmert M,
1113 Söding J, Thompson JD, Higgins DG. (2011) Fast, scalable generation of high-quality protein
1114 multiple sequence alignments using Clustal Omega. Mol Syst Biol. 7:539. doi:
1115 10.1038/msb.2011.75.

1116
1117 Skelly PJ, Da'dara AA, Li X-H, Castro-Borges W, Wilson RA (2014) Schistosome feeding and
1118 regurgitation. PLoS Pathog 10(8): e1004246. doi.org/10.1371/journal.ppat.1004246
1119
1120 Skinner DE, Rinaldi G, Suttiprapa S, Mann VH, Smircich P, Cogswell AA, Williams DL, Brindley
1121 PJ. Vasa-Like DEAD-Box RNA Helicases of *Schistosoma mansoni*. PLoS Negl Trop Dis.
1122 2012;6(6):e1686. doi: 10.1371/journal.pntd.0001686.
1123
1124 Smit CH, van Diepen A, Nguyen DL, Wuhrer M, Hoffmann KF, Deelder AM, Hokke CH (2015)
1125 Glycomic analysis of life stages of the human parasite *Schistosoma mansoni* reveals developmental
1126 expression profiles of functional and antigenic glycan motifs. Molecular & Cellular Proteomics 14,
1127 7: 1750-1769. doi.org/10.1074/mcp.M115.048280.
1128
1129 Sonoda J, Mehl IR, Chong LW, Nofsinger RR, Evans RM. PGC-1beta controls mitochondrial
1130 metabolism to modulate circadian activity, adaptive thermogenesis, and hepatic steatosis. Proc Natl
1131 Acad Sci U S A. 2007;104:5223–5228.
1132
1133 Stice, J.P., Knowlton, A.A. Estrogen, NFκB, and the heat shock response. *Mol Med* 14, 517–527
1134 (2008). https://doi.org/10.2119/2008-00026.
1135
1136 Stuart T, Butler A, Hoffman P, Hafemeister C, Papalexi E, Mauck WM, Hao Y, Stoeckius M,
1137 Smibert P, Satija R (2019) Comprehensive integration of single-cell data. Cell;177(7):1888-
1138 1902.e21.doi: 10.1016/j.cell.2019.05.031.
1139
1140 Szklarczyk D, Gable AL, Lyon D, Junge A, Wyder S, Huerta-Cepas J, Simonovic M, Doncheva
1141 NT, Morris JH, Bork P, Jensen LJ, von Mering C (2019) STRING v11: protein–protein association
1142 networks with increased coverage, supporting functional discovery in genome-wide experimental
1143 datasets, Nucleic Acids Research. 47:607–613, https://doi.org/10.1093/nar/gky1131
1144
1145 Takahashi J (2017) Transcriptional architecture of the mammalian circadian clock. *Nat Rev Genet*
1146 18, 164–179. https://doi.org/10.1038/nrg.2016.150
1147
1148 Tissières A, Mitchell HK, Tracy UM. (1974) Protein synthesis in salivary glands of *Drosophila*
1149 *melanogaster:* relation to chromosome puffs. J Mol Biol. 84(3):389-98. doi: 10.1016/0022-
1150 2836(74)90447-1.
1151
1152 Tsoumtsa LL, Torre C, Trouplin V, Coiffard B, Gimenez G, Mege JL, Ghigo E. Antimicrobial
1153 capacity of the freshwater planarians against *S. aureus* is under the control of Timeless. Virulence.
1154 2017 Oct 3;8(7):1160-9.
1155
1156 Vogel JL, Parsell DA, Lindquist S. (1995) Heat-shock proteins Hsp104 and Hsp70 reactivate
1157 mRNA splicing after heat inactivation. Curr Biol. 5(3):306-17. doi: 10.1016/s0960-9822(95)00061-
1158 3.
1159
1160 Wang B, Lee J, Li P, Saberi A, Yang H, Liu C, Zhao M, Newmark PA(2018) Stem cell
1161 heterogeneity drives the parasitic life cycle of *Schistosoma mansoni.* eLife 2018;7:e35449 DOI:
1162 10.7554/eLife.35449
1163
1164 Wang J, Chen R, Collins JJ III (2019) Systematically improved *in vitro* culture conditions reveal
1165 new insights into the reproductive biology of the human parasite *Schistosoma mansoni.* PLoS Biol
1166 17(5): e3000254. doi.org/10.1371/journal.pbio.3000254

1167 Wang J, Paz C, Padalino G, Coghlan A, Lu Z, Gradinaru I, Collins JNR, Berriman M, Hoffmann
1168 KF, Collins JJ III (2020) Large-scale RNAi screening uncovers therapeutic targets in the parasite
1169 *Schistosoma mansoni*. Science 369:1649-1653. DOI: 10.1126/science.abb7699

1170 Waterhouse AM, Procter JB, Martin DM, Clamp M, Barton GJ. (2009) Jalview Version 2—a
1171 multiple sequence alignment editor and analysis workbench. Bioinformatics.25(9):1189-91.
1172
1173 Wen S, Ma D, Zhao M, Xie L, Wu Q, Gou L, Zhu C, Fan Y, Wang H, Yan J. (2020)
1174 Spatiotemporal single-cell analysis of gene expression in the mouse suprachiasmatic nucleus. Nat
1175 Neurosci. 23(3):456-467. doi: 10.1038/s41593-020-0586-x.
1176
1177 Wendt G, Zhao L, Chen R, Liu C, O'Donoghue AJ, Caffrey CR, Reese ML, Collins JJ III (2020) A
1178 single-cell RNA-seq atlas of *Schistosoma mansoni* identifies a key regulator of blood feeding.
1179 Science 369, 1644–1649. DOI: 10.1126/science.abb7709
1180
1181 Westwood ML, O'Donnell AJ, de Bekker C, Lively CM , Zuk M, Reece SE (2019) The
1182 evolutionary ecology of circadian rhythms in infection. *Nat Ecol Evol* 3, 552–560.
1183 https://doi.org/10.1038/s41559-019-0831-4
1184
1185 Whitmore D, Foulkes NS, Strähle U, Sassone-Corsi P (1998) Zebrafish Clock rhythmic expression
1186 reveals independent peripheral circadian oscillators. Nat Neurosci. 1998 Dec;1(8):701-7. doi:
1187 10.1038/3703.
1188
1189 Wu G, Anafi RC, Hughes ME, Kornacker K, Hogenesch JB (2016) MetaCycle: an integrated R
1190 package to evaluate periodicity in large scale data Bioinformatics 32(21):3351-3353. doi:
1191 10.1093/bioinformatics/btw405.
1192
1193 Xu F, Kula-Eversole E, Iwanaszko M, Hutchison AL, Dinner A, Allada R (2019) Circadian Clocks
1194 Function in Concert with Heat Shock Organizing Protein to Modulate Mutant Huntingtin
1195 Aggregation and Toxicity, Cell Reports, 27, 59-70.e4, https://doi.org/10.1016/j.celrep.2019.03.015.
1196
1197 Yang J, Zhang Y (2015) I-TASSER server: new development for protein structure and function
1198 predictions. Nucleic Acids Research, 43: W174-W181
1199
1200 You H, Gobert GN, Duke MG, Zhang W, Li Y, Jones MK, McManus DP (2012) The insulin
1201 receptor is a transmission blocking veterinary vaccine target for zoonotic *Schistosoma japonicum.*
1202 International Journal for Parasitology 42;801-807 doi.org/10.1016/j.ijpara.2012.06.002
1203
1204 You H, Gobert GN, Cai P, Mou R, Nawaratna S, Fang G, Villinger F, McManus DP (2015)
1205 Suppression of the insulin receptors in adult *Schistosoma japonicum* impacts on parasite growth and
1206 development: further evidence of vaccine potential. PLoS Negl Trop Dis 9(5): e0003730.
1207 https://doi.org/10.1371/journal.pntd.0003730
1208
1209 Zantke J, Ishikawa-Fujiwara T, Arboleda E, Lohs C, Schipany K, Hallay N, Straw AD, Todo T,
1210 Tessmar-Raible K. (2013) Circadian and circalunar clock interactions in a marine annelid. Cell Rep.
1211 5(1):99-113. doi: 10.1016/j.celrep.2013.08.031.
1212
1213 Zhang R, Lahens NF, Balance HI, Hugher ME, Hogenesch JB (2014) A circadian gene expression
1214 atlas in mammals: implications for biology and medicine. PNAS 111:16219-16224.
1215 doi.org/10.1073/pnas.1408886111
1216

Zheng X, Sehgal A. (2008) Probing the relative importance of molecular oscillations in the circadian clock. Genetics. 178(3):1147-55. doi: 10.1534/genetics.107.088658.

Zhu H, Sauman I, Yuan Q, Casselman A, Emery-Le M, Emery P, Reppert SM (2008) Cryptochromes define a novel circadian clock mechanism in monarch butterflies that may underlie sun compass navigation. PLoS Biol. 6(1):e4. doi: 10.1371/journal.pbio.0060004.

Supplementary figures

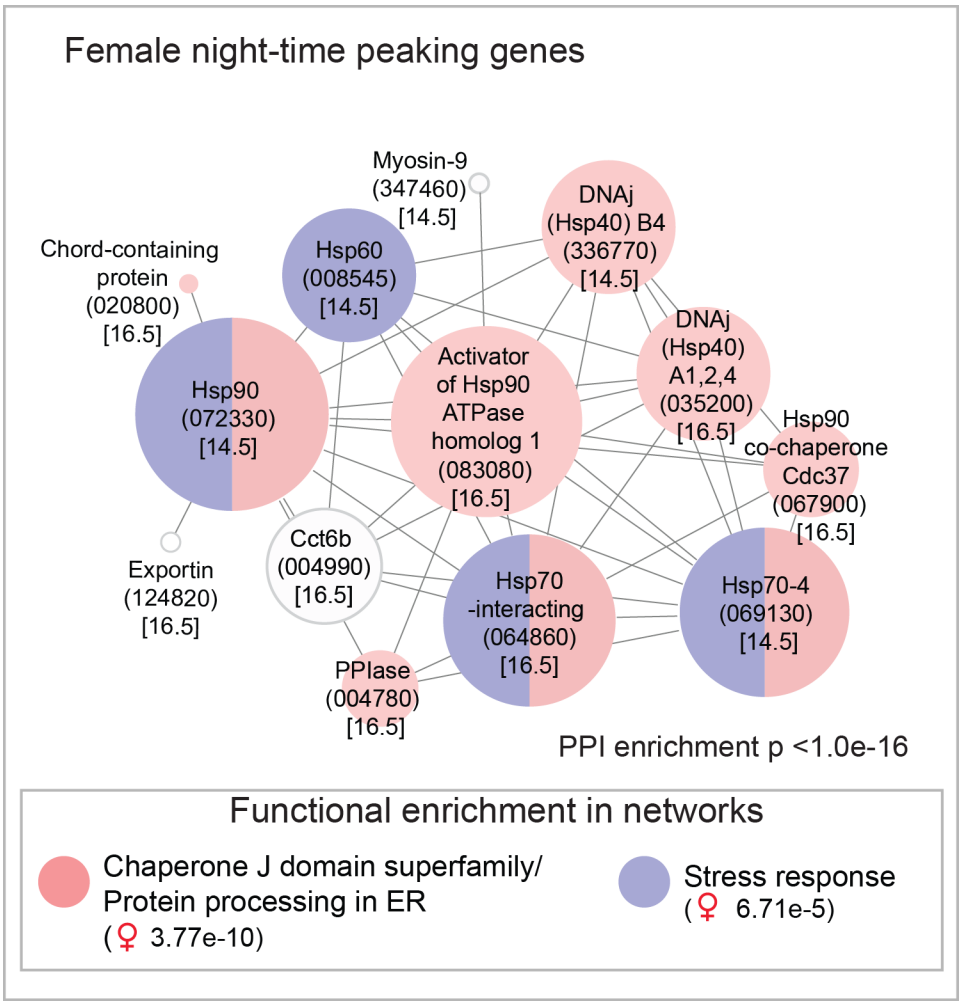

Supplementary figure 1. Predicted molecular interaction networks of night-time peaking genes in female *Schistosoma mansoni* (computed using the STRING online database). Node size reflects the number of connections a molecule has within the network. Lines (edges) connecting nodes are based on evidence of the function of homologues. Functional enrichment (FDR) as provided by STRING. (PPI= predicted protein interaction; geneIDs with Smp_ prefixes removed; acrophase in brackets).

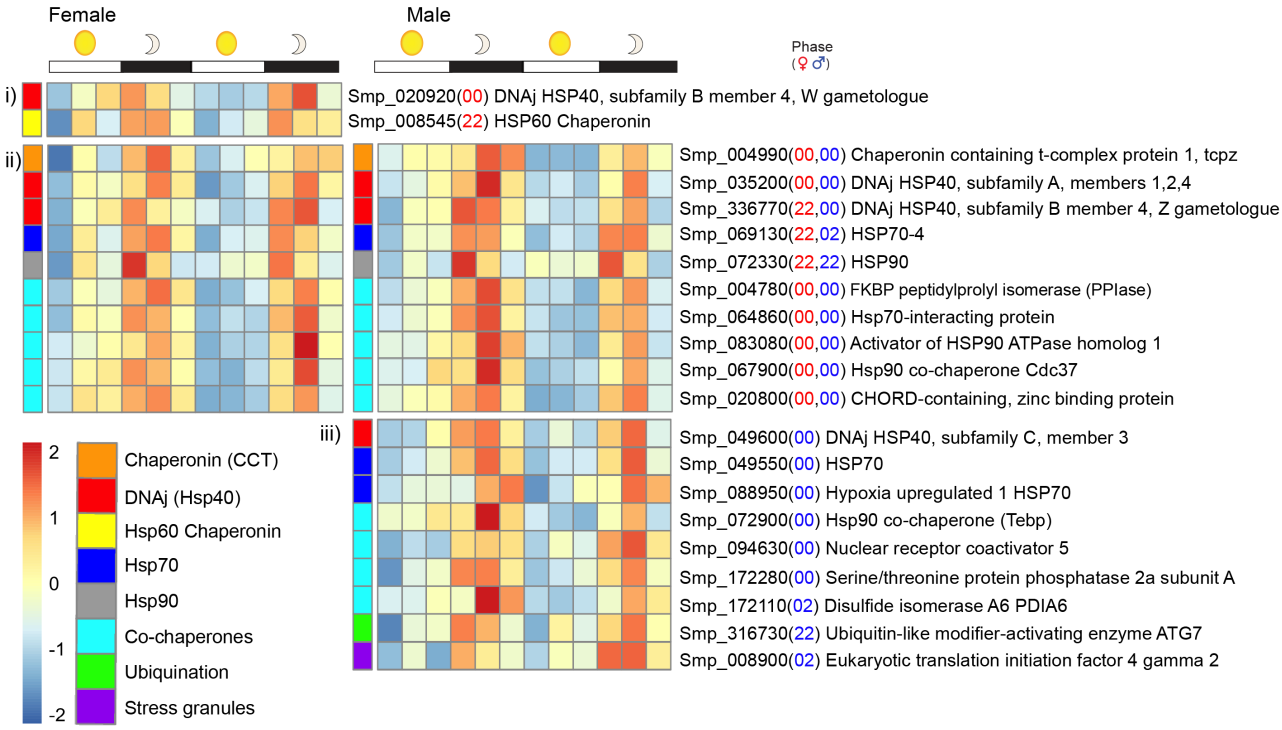

Supplementary figure 2. Diel genes encoding heat shock proteins, co-chaperones and other proteins involved in heat shock response and recovery. All reach their acrophase between 22:00-02:00 hours but some show diel expression in one sex only (i & iii), whereas another ten cycle in both sexes, with eight in phase (ii).

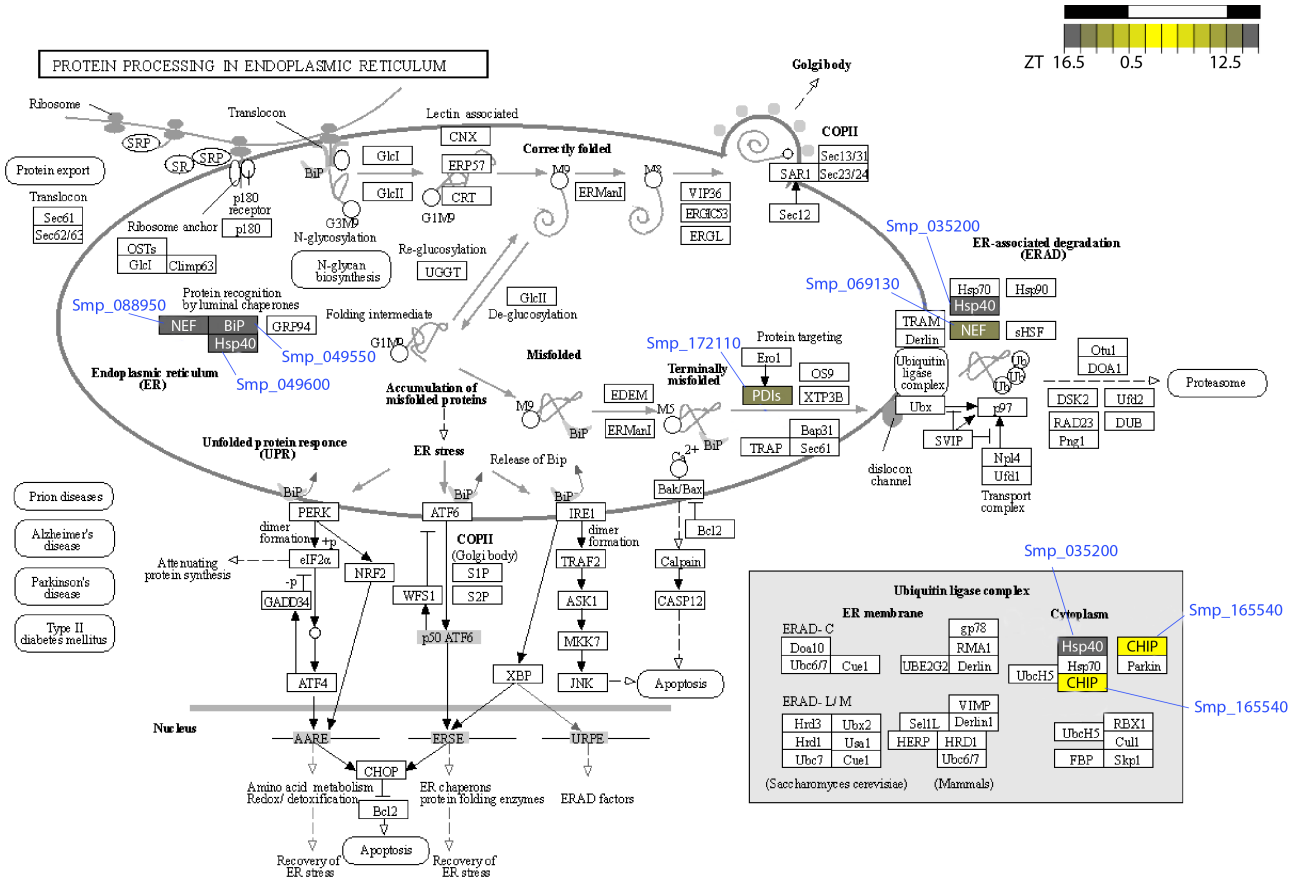

Supplementary figure 3. The KEGG pathway 'Protein processing in endoplasmic reticulum' includes seven diel genes that encode heat shock proteins and other co-chaperones. Data on KEGG graph rendered by Pathview.

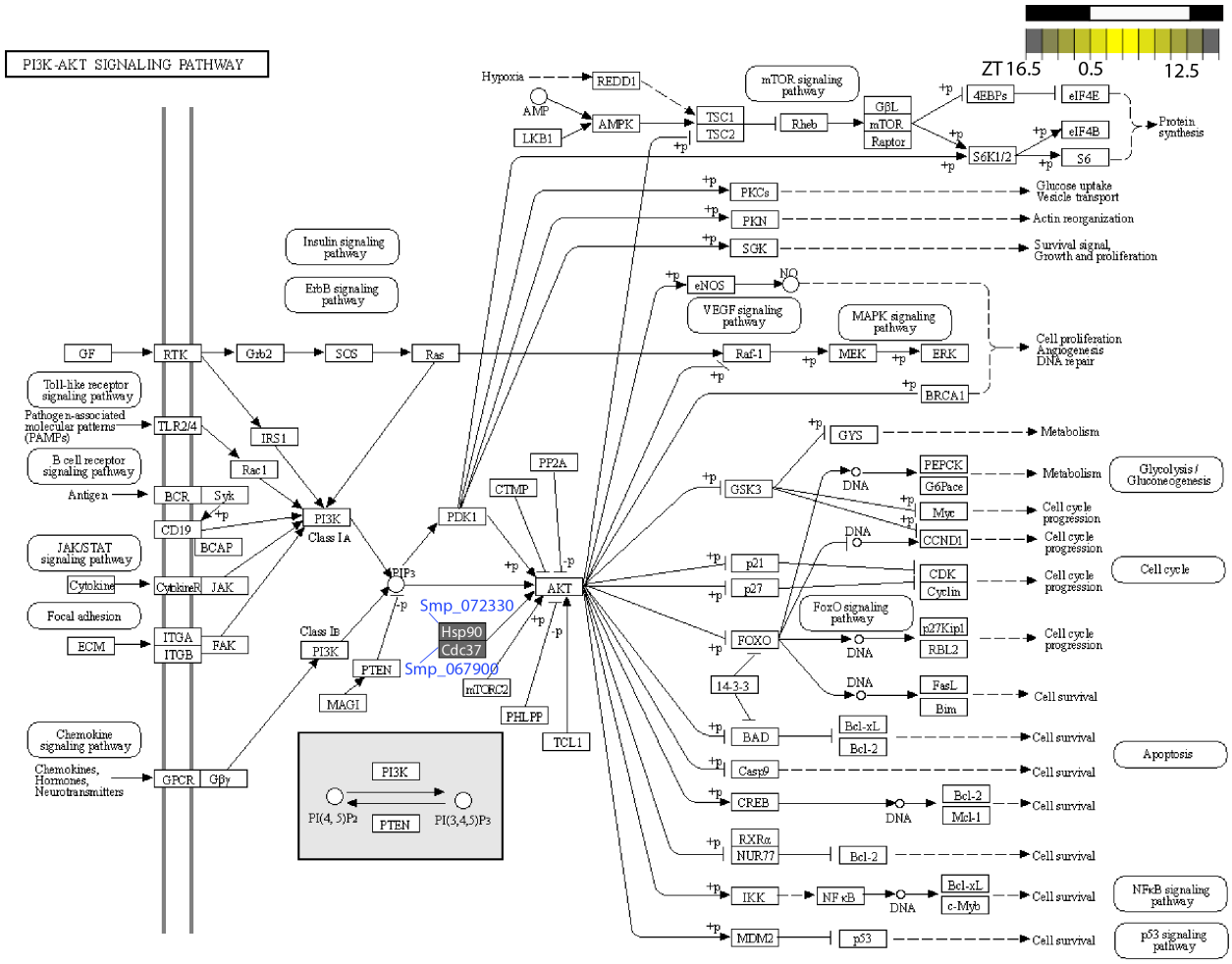

Supplementary figure 4. The KEGG pathway 'PI3K-AKT signaling pathway' includes two diel genes; one that encodes heat shock protein 90 (HSP90) and the other encodes one of its co-chaperones, cell division cycle 37 (Cdc37). Data on KEGG graph rendered by Pathview.

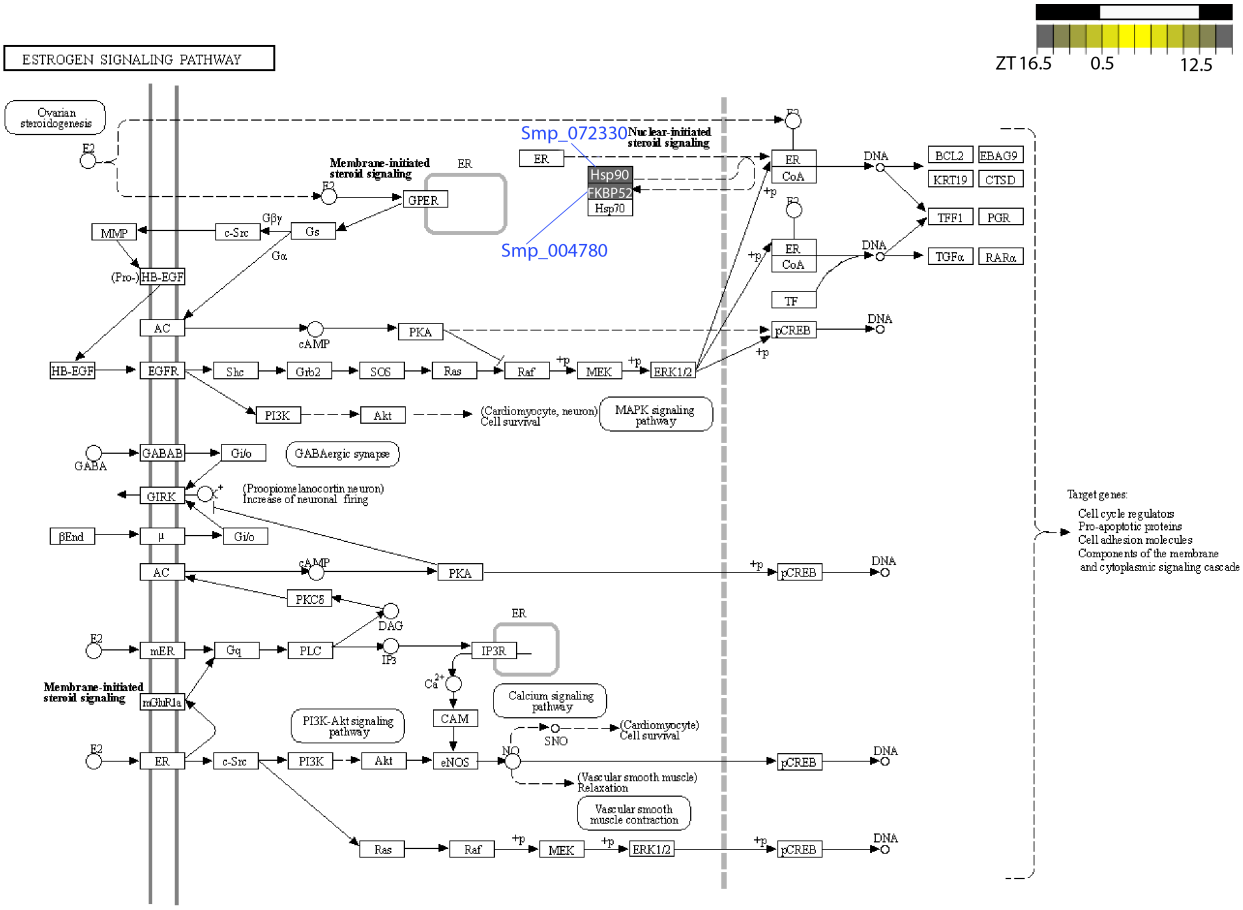

Supplementary figure 5. The KEGG pathway 'Estrogen signaling pathway' includes two diel genes; one that encodes heat shock protein 90 (HSP90) and the other encodes one of its co-chaperones, immunophilin (FKBP52). However, HSP70 (Smp_303420), another binding partner, does not cycle in male or female worms. Data on KEGG graph rendered by Pathview.

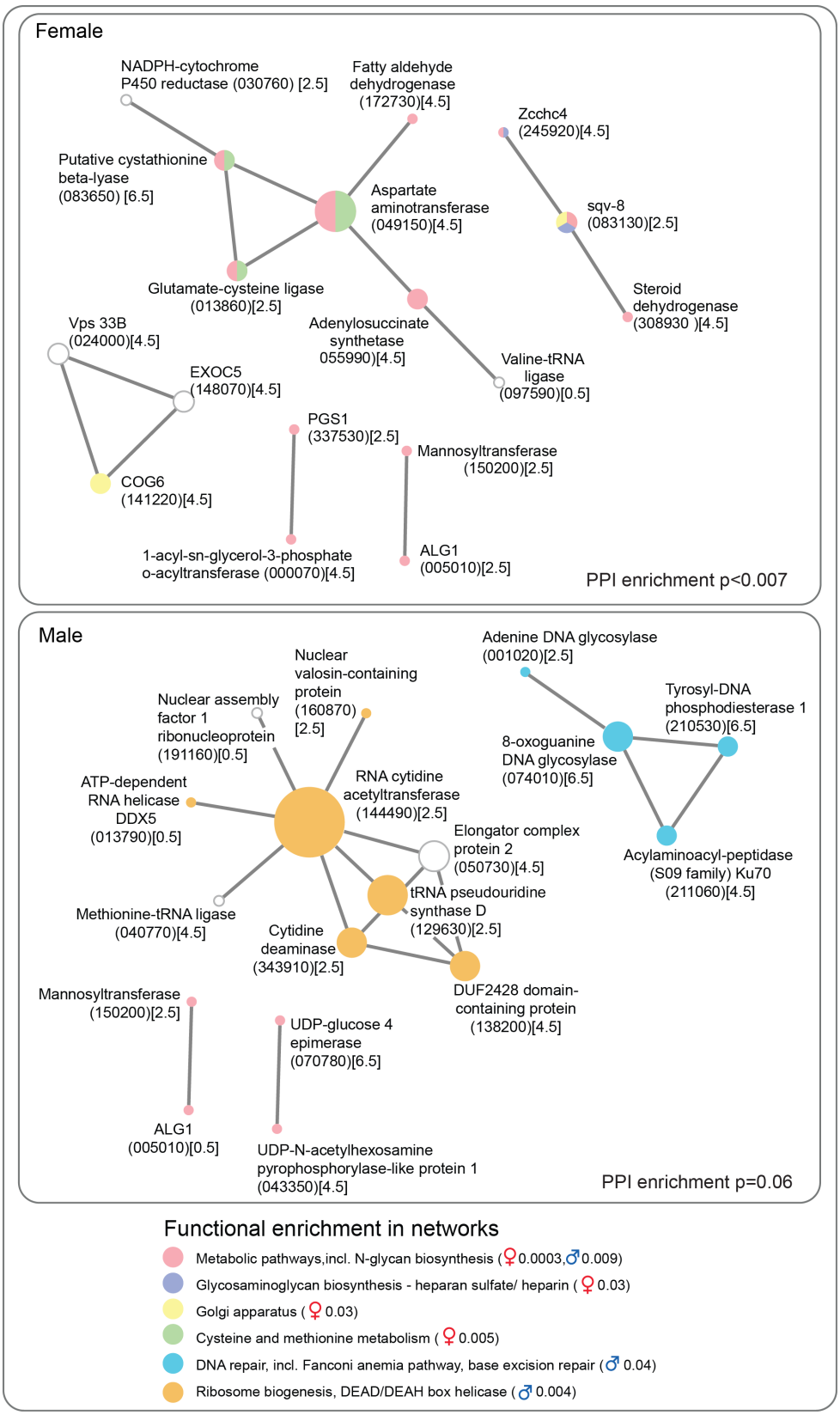

Supplementary figure 6. Predicted molecular interaction networks of day-time peaking genes in female and male *Schistosoma mansoni* (computed using the STRING online database). Node size reflects the number of connections a molecule has within the network. Lines (edges) connecting nodes are based on evidence of the function of homologues. Functional enrichment (FDR) as provided by STRING. (PPI= predicted protein interaction; "Smp_" prefixes have been removed from gene identifiers for clarity; acrophase in brackets).

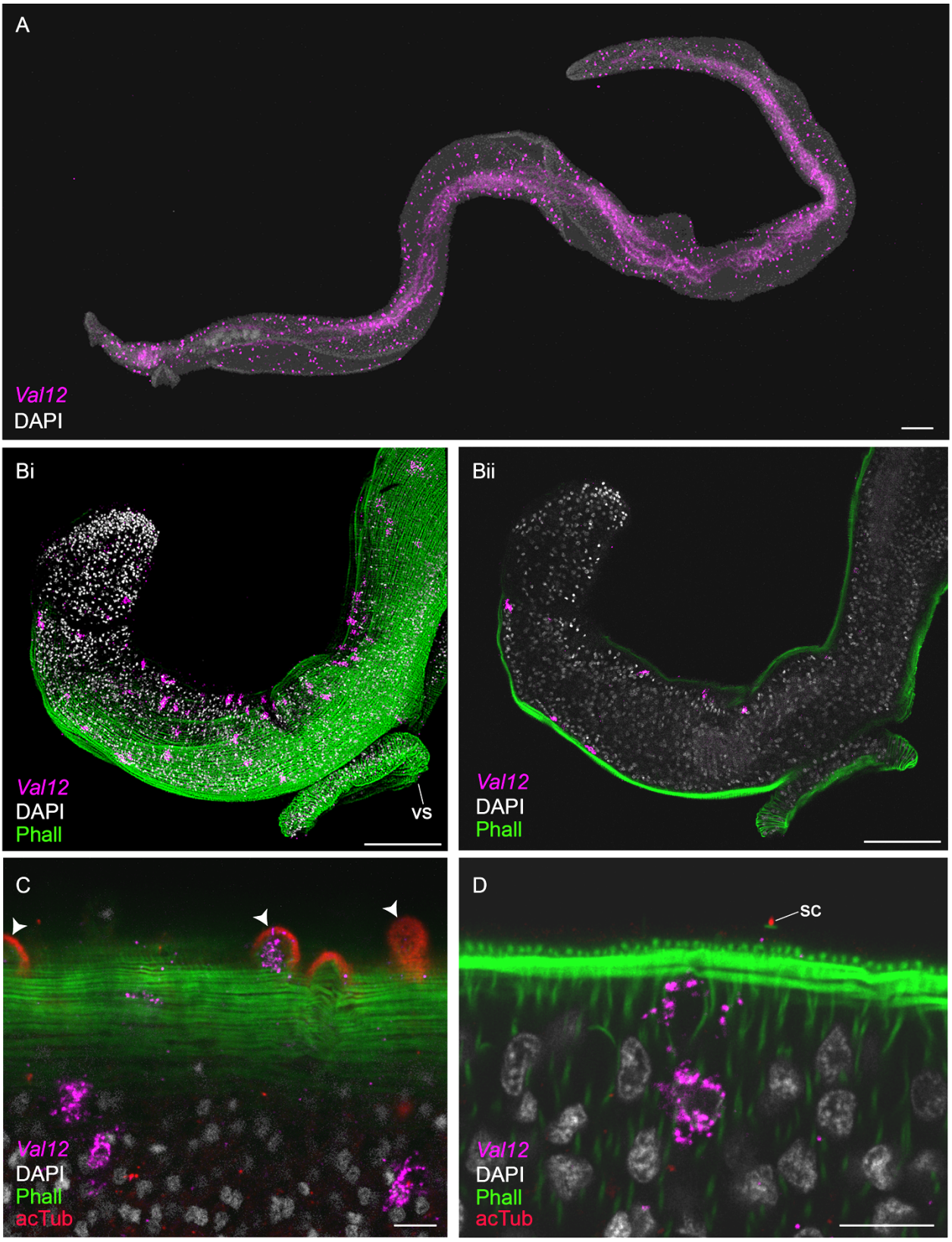

Supplementary figure 7. In male worms *Venom allergen-like 12* (*Val12*, Smp_123540) transcripts peak in abundance at midday (ZT 4.5) and are expressed in **A)** ~ 500 cells that are distributed the length of the body (anterior to left)(scale = 200µm). **B)** The *Val12*$^{+}$ cells sit below the body wall musculature (phall = phalloidin) on both the ventral and dorsal sides, **i**) 3D projection and **ii**) optical section of the head (scale = 100µm). **C&D**) *Val12* is expressed in some tubercles (arrowhead) of the dorsal tegument, as well as directly under the body wall musculature (scale = 10µm)(optical

sections)(acTub = acetylated tubulin).vs = ventral sucker, sc = sensory cilia. 100% of individuals examined, n = 20.

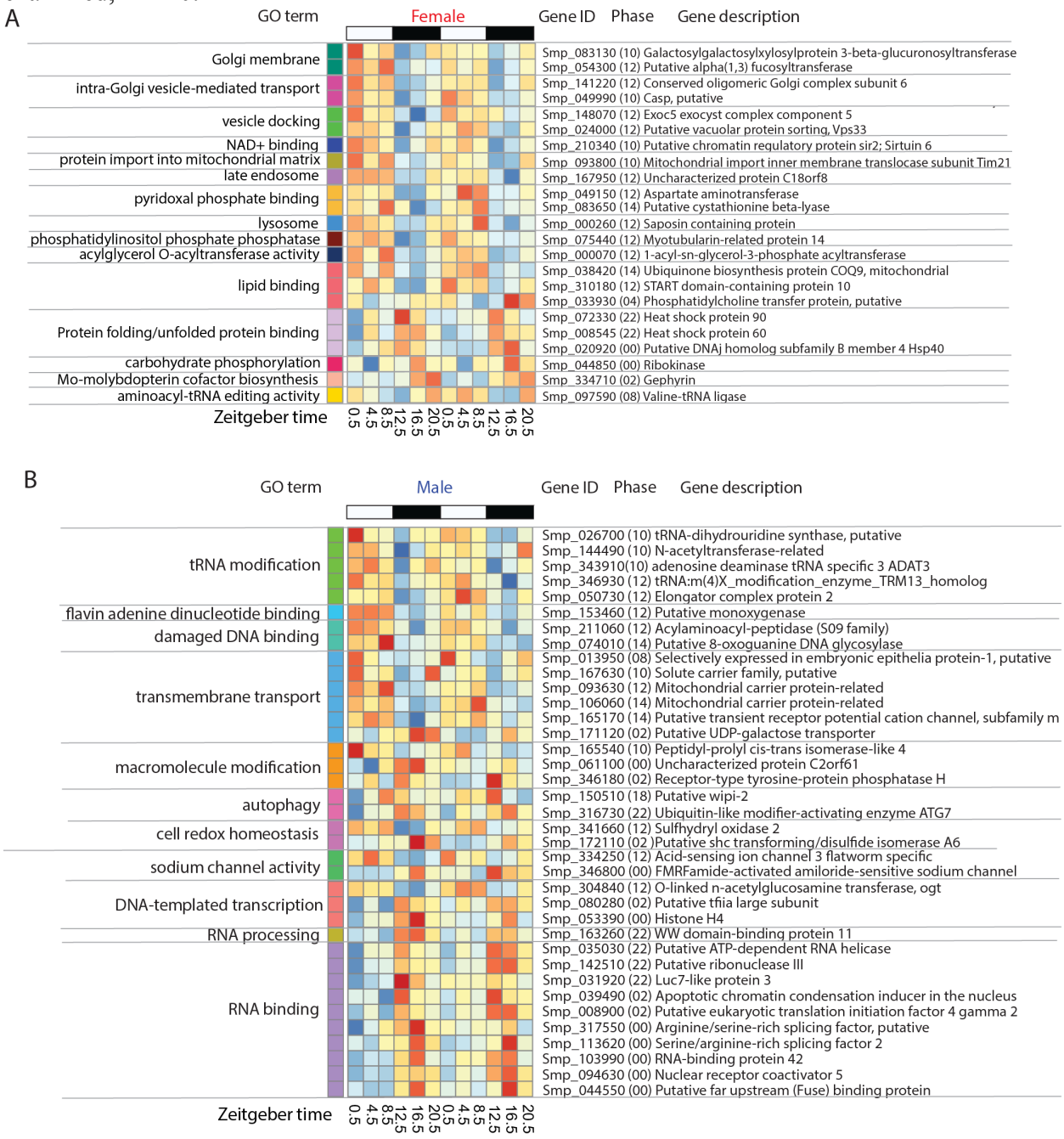

Supplementary figure 8. Sex-specific 24-hour rhythmic processes. Heatmaps showing GO terms enriched in diel genes that cycle in females (**A**) or males (**B**) only.

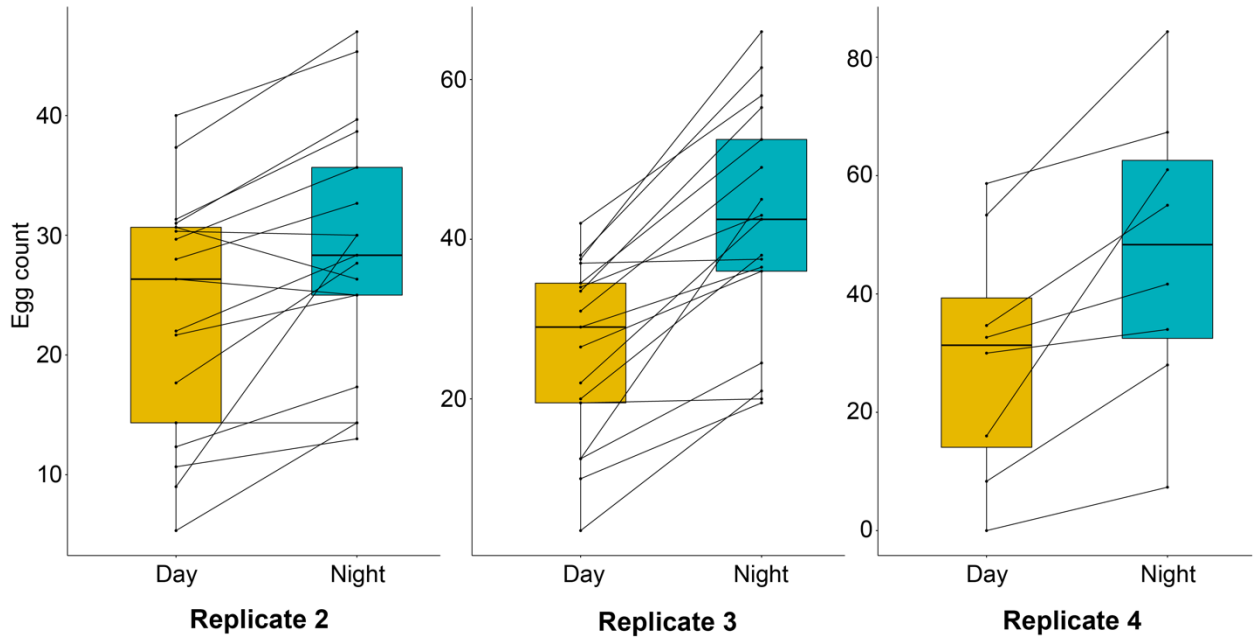

Supplementary figure 9. Independent biological replicates of day and night egg counts from paired female worms *in vitro* (median and interquartile ranges). Replicate 2: n=17, paired Wilcoxon test P=0.002, median(night-day)=5.3. Replicate 3: n=17, P=0.0003, median(night-day)=17.5. Replicate 4: n=8, P=0.008, median(night-day)=14.3.

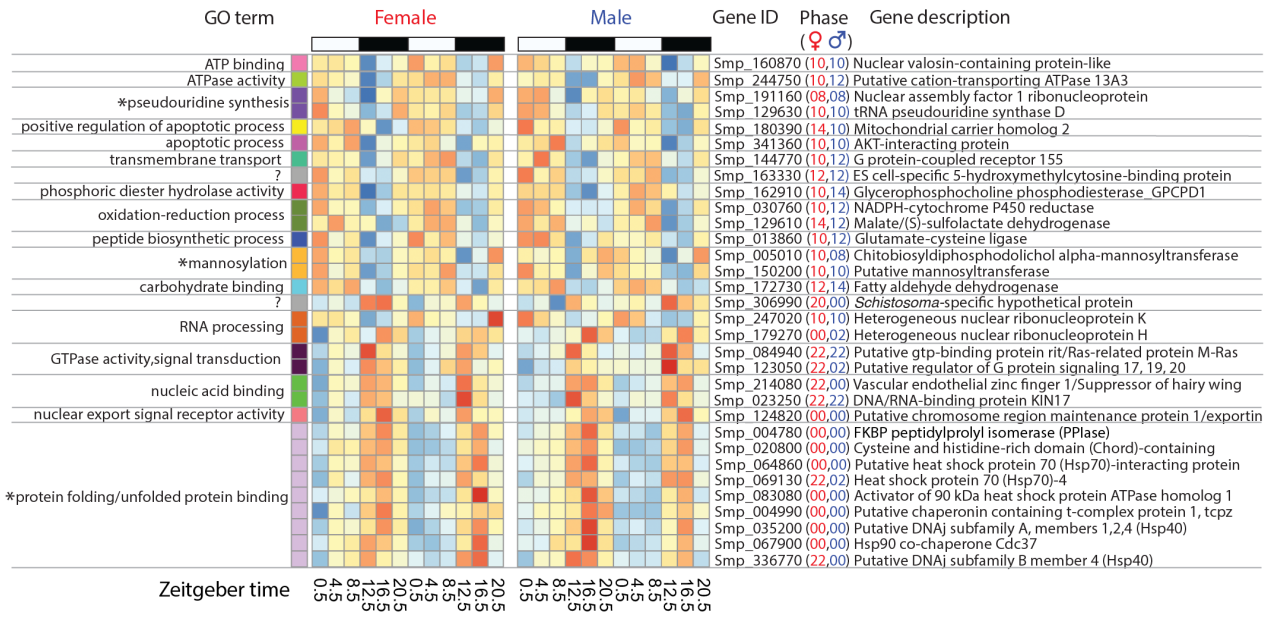

Supplementary figure 10. Diel genes common to female and male worms show identical, or similar, phases suggesting that many biological processes and molecular functions (GO terms) are happening in synchrony. Most enriched functions are time-of-day specific; e.g. mannosylation, redox homeostasis and apoptosis occur during the daytime, whereas genes involved in molecular chaperoning, nucleic acid binding and signal transduction reach their acrophase at night. (* significantly enriched GO terms FDR<0.01, **supplementary table 5**).

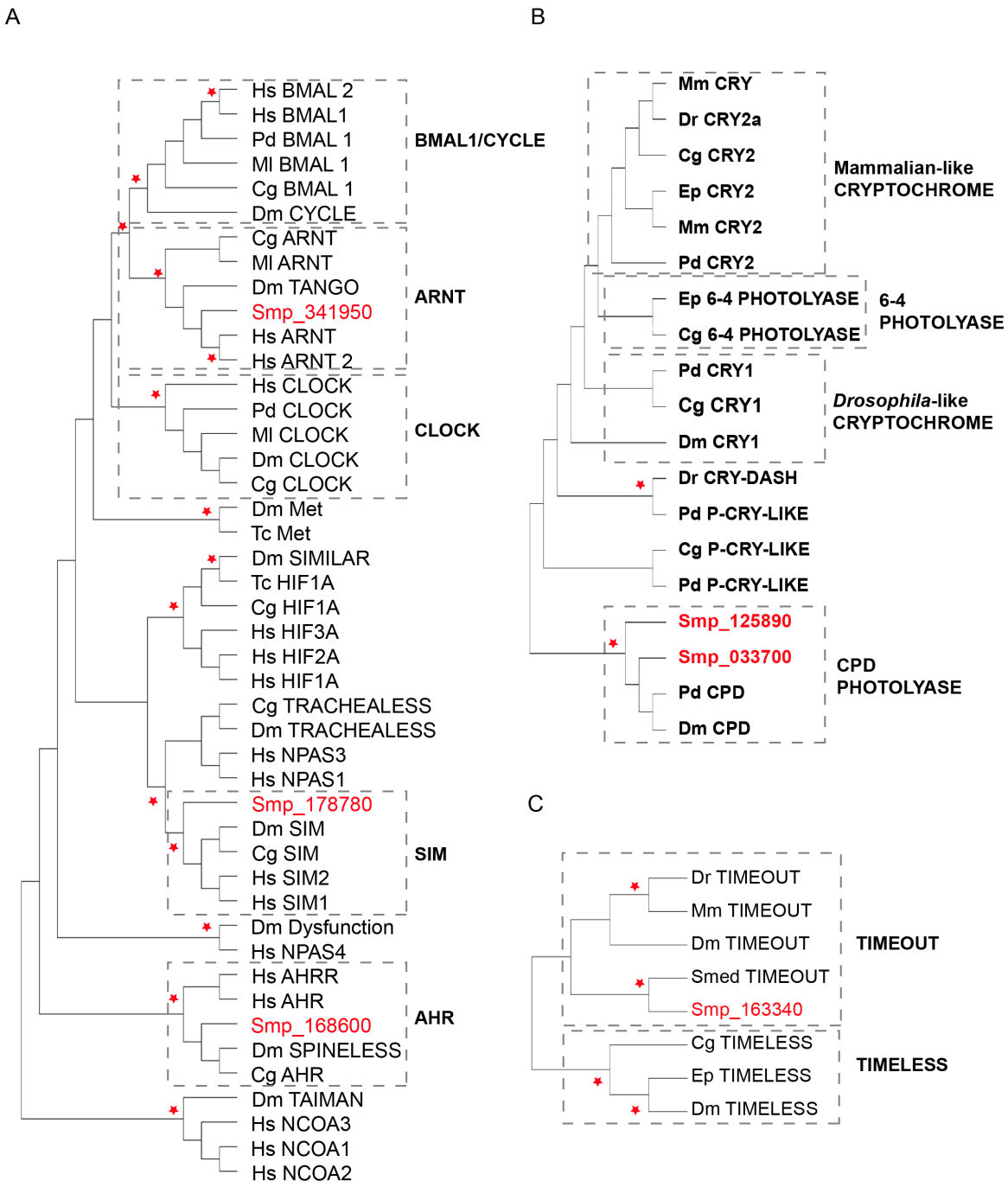

Supplementary figure 11. Core circadian clock gene homologs are missing in *Schistosoma mansoni*. Neighbour-joining phylogenetic trees were constructed in Mega-X with 1000 bootstrap replications and partial/pairwise deletion (* = bootstrap support >90). **A**) A phylogeny of bHLH/PAS domain proteins shows that *S.mansoni* lacks BMAL1 and CLOCK homologs. Our BLASTP hits cluster with the closely-related non-circadian proteins ARNT, AHR and SIM. **B**) A phylogeny of orthologous genes *tim1* (TIMELESS) and *tim2* (TIMEOUT) shows that our BLASTP hit clusters with *tim2*. We also show that the previously identified *timeless* homolog in the flatworm *Schmidtea mediterreana* (Tsoumtsa et al., 2017) clusters with *tim2* homologs of model organisms. **C**) *S. mansoni* has two CPD photolyases but no circadian-related Cryptochromes. Abbreviations: Cg = *Crassostrea gigas*, Dr = *Danio rerio,* Dm = *Drosophila melanogaster,* Ep = *Eurydice pulchra*, Hs = *Homo sapiens,* Ml = *Melibe leonina*, *Mm = Mus musculus,* Pd = *Platynereis dumerilii*, Smed = *Schmidtea mediterranea*, Tc = *Tribolium castaneum*

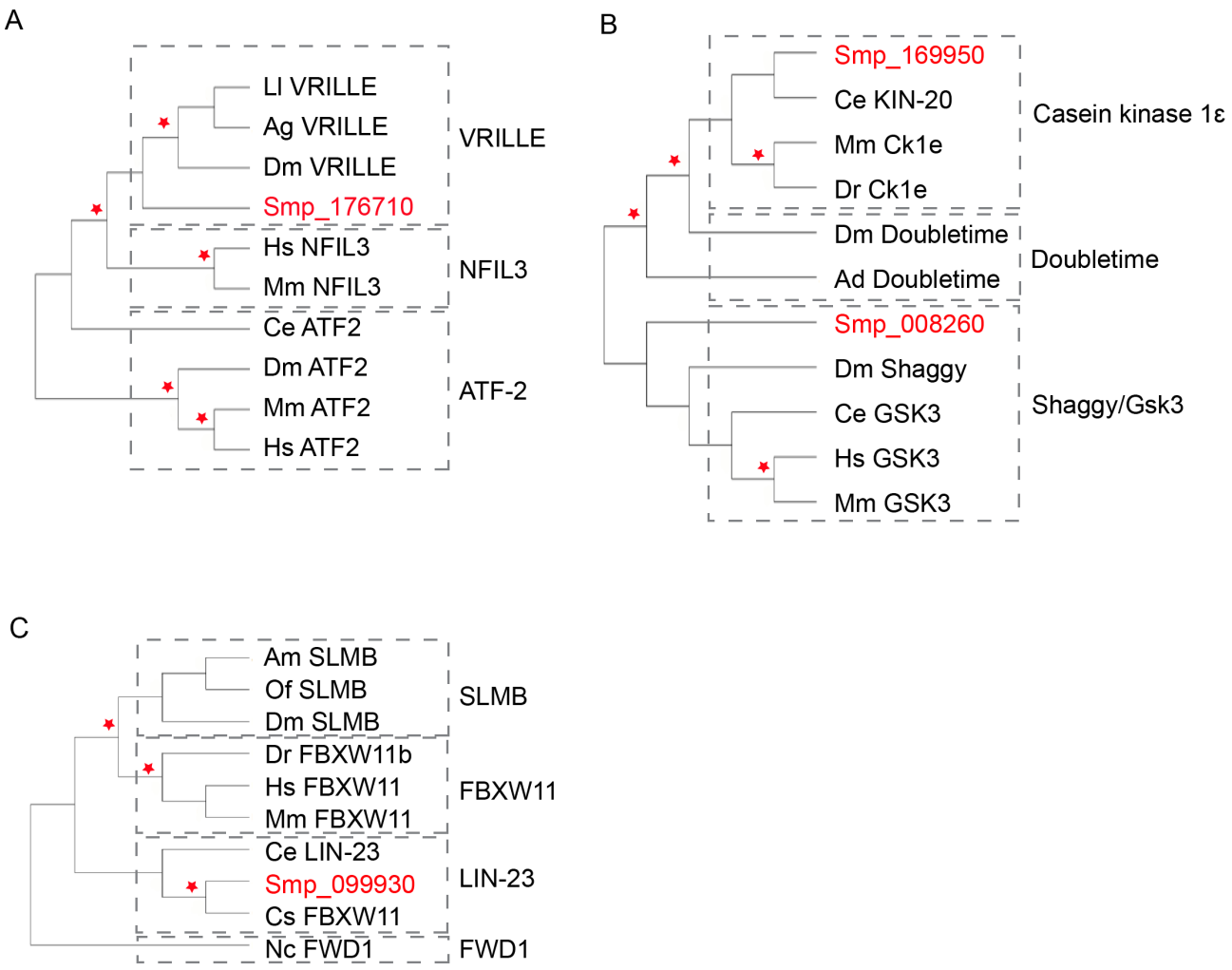

Supplementary figure 12. *Schistosoma mansoni* has homologs of secondary clock genes. Neighbour-joining phylogenetic trees were constructed in Mega-X with 1000 bootstrap replications and 80% partial deletion using sequences obtained from Uniprot. (* = bootstrap support >90). **A**) Representatives of basic-leucine zipper protein family show insect *vrille* homolog is present in *S. mansoni*. **B**) Smp_169950 clusters with mammalian homologs of *doubletime*, whereas Smp_008260 clusters with *Shaggy*. **C**) Smp_099930 clusters with Lin-23, a previously identified homolog of Slmb in *Caenorhabditis elegans*. Ancestral sequence from *Neurospora Crassa* was used as an out-group. Conserved regions were obtained in Gblocks using least stringency criteria and percentage of all sequences used was as follows: 3% basic-leucine zipper, 11% slmb, 18% shaggy/doubletime. Abbreviations: Ll = *Lutzomyia longipalpis*, Ag = *Anopheles gambiae*, Dm = *Drosophila melanogaster*, Hs = *Homo sapiens*, Mm = *Mus musculus*, Ce = *Caenorhabditis elegans*, Cg = *Crassostrea gigas,* Am = *Apis mellifera*, Of = *Oncopeltus fasciatus* , Dr = *Danio rerio*, Nc = *Neurospora crassa*, Cs = *Clonorchis sinensis*, Ad = *Anopheles darlingi.*